Absorbing boundary conditions for the two-dimensional Schrödinger equation with an exterior potential. Part II: discretization and numerical results

Xavier ANTOINE

Institut Elie Cartan Nancy, Université de Lorraine,
CNRS UMR 7502, INRIA CORIDA Team,
Boulevard des Aiguillettes B.P. 239,
F-54506 Vandoeuvre-lès-Nancy, France

`Xavier.Antoine@iecn.u-nancy.fr`

Christophe BESSE

Laboratoire Paul Painlevé, Université Lille Nord de France,
CNRS UMR 8524, INRIA SIMPAF Team,
Université Lille 1 Sciences et Technologies, Cité Scientifique,
59655 Villeneuve d'Ascq Cedex, France.

`Christophe.Besse@math.univ-lille1.fr`

Pauline KLEIN

Laboratoire de Mathématiques de Besançon,
CNRS UMR 6623, Université de Franche-Comté,
16 route de Gray, 25030 Besançon, France.

`Pauline.Klein@univ-fcomte.fr`.

Abstract

Four families of ABCs where built in [6] for the two-dimensional linear Schrödinger equation with time and space dependent potentials and for general smooth convex fictitious surfaces. The aim of this paper is to propose some suitable discretization schemes of these ABCs and to prove some semi-discrete stability results. Furthermore, the full numerical discretization of the corresponding initial boundary value problems is considered and simulations are provided to compare the accuracy of the different ABCs.

Key words: Schrödinger equation; absorbing boundary conditions; variable potential.

AMS Subject Classification: 35Q41, 47G30, 35S15

1. Introduction

The aim of this paper is to propose accurate and stable discretizations to some Absorbing Boundary Conditions (ABCs) for the two-dimensional linear

March 2012

time-dependent Schrödinger equation [2] with a general potential V

$$\begin{cases} i\partial_t u + \Delta u + V(x,y,t)u = 0, & (x,y) \in \mathbb{R}^2, t > 0 \\ u(x,y,0) = u_0(x,y), & (x,y) \in \mathbb{R}^2, \end{cases} \tag{1}$$

where $u_0 \in L^2(\mathbb{R}^2)$ is compactly supported in the future bounded spatial computational domain Ω, with fictitious boundary Σ. The potential function is C^∞, space and time dependent and real-valued. We assume that V is a smooth potential outside the computational domain $\Omega_T = \Omega \times]0;T[$, T being the final time of computation. We also introduce $\Sigma_T := \Sigma \times]0;T[$. Under suitable conditions, the initial boundary value problem (1) is well-posed [8, 9]. Moreover, the L^2-norm of the solution is conserved in the free-space

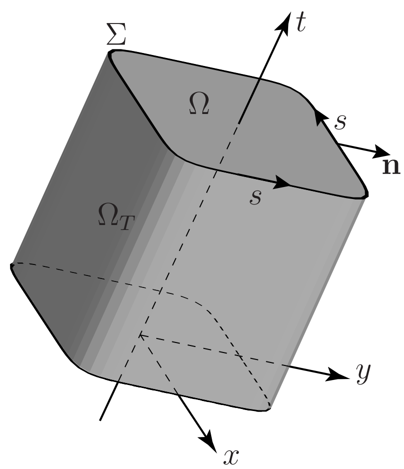

Figure 1: Geometry

$$\forall t > 0, \quad \|u(t)\|^2_{L^2(\mathbb{R}^2)} = \int_{\mathbb{R}^2} |u(x,y,t)|^2 dxdy = \|u_0\|^2_{L^2(\mathbb{R}^2)}, \tag{2}$$

where $\|\cdot\|^2_{L^2(\mathbb{R}^2)}$ is the $L^2(\mathbb{R}^2)$-norm. Finally, $\mathbf{n}$ is the outwardly directed unit normal vector to Σ. In practical applications, considering potential effects is a crucial and active topic that is not completely well managed in physics [10, 11, 19, 20, 23].

Absorbing Boundary Conditions are used in practical computations when an unbounded domain has to be truncated for computational purposes. When a wave strikes the fictitious boundary Σ that is introduced for the numerical solution, and when this wave should be outgoing to the bounded computational domain Ω, the aim of the ABC is to minimize the reflection back into the computational domain that is generated by Σ. When there is no reflection at all, the boundary condition is generally called "Transparent Boundary Condition (TBC)". Nevertheless, such a boundary condition is generally out of reach, most particularly in our situation. For this reason, ABCs, which are approximations of the TBC, are generally preferred since mathematical techniques can be developed to obtain such approximations. For a very complete and global overview of these different approaches we refer to [2]. From the point of view of ABCs and for the problem considered in this paper, absorbing boundary conditions for some particular time independent one-dimensional potentials can be obtained by using explicit expressions of the Dirichlet-to-Neumann (DtN) operator through special functions (for example Airy's functions) [17, 18] or adapted techniques (Floquet's theory for sinusoidal potentials [24]).

In a first part [6], we derived (under a high frequency assumption) different kinds of ABCs by using some adaptations of pseudodifferential operators techniques introduced in the fundamental papers [13, 15] by Engquist & Majda. Based on symbolic calculus associated with some special fractional pseudodifferential operators, this method allows us to build asymptotic expansions of the total symbols for the underlying pseudodifferential operators. This leads to two classes of ABCs according to two possible constructive strategies. The first family of ABCs (obtained by Strategy I in the sequel of the paper, and also in [6]) is associated with a Schrödinger-like equation after a gauge change has been applied. The second approach, that we call Strategy II, consists in directly building ABCs for the initial Schrödinger equation of system (1). The ABCs are defined through approximations of the exact Dirichlet-to-Neumann map which are nonlocal both in space and time. This constraint is very restrictive for an effective calculation since this leads to additional memory costs and long computational times. One natural way to overcome this problem is to suitably localize the involved nonlocal operators. Therefore, each family of ABCs is approximated by using Taylor's or Padé's expansions of the symbols. This results in four types of ABCs. Well-posedness of the associated initial boundary value problems have been obtained in [6] for some of the proposed ABCs. We can then expect some similar properties at the discrete level to prove that the related schemes are unconditionally stable. The aim of this paper is to propose some discretization schemes of the ABCs derived in [6] and to prove when possible some stability results. Furthermore, through numerical simulations on nontrivial cases, we want to compare the different ABCs in terms of accuracy and efficiency.

The paper is organized as follows. In the second Section, we explain the main ingredients concerning the construction of absorbing boundary conditions and give the four families of ABCs obtained in [6]. In Section 3, we consider semi discretizations in time based on the Crank-Nicolson scheme. We explain how to obtain suitable discrete schemes adapted to the approximation of the different kinds of ABCs. In particular, stability results are proved under a semi-discrete high frequency assumption. Section 4 deals with the full numerical approximation and finite element implementation of the ABCs. This part is completed with various computations to analyze and compare the accuracy of the different ABCs for time independent and time dependent potentials. We draw a conclusion in Section 5. Finally, Annex A provides some technical details about the $\mathcal{Z}$-transform which plays a central role in the proofs of the paper.

2. Four families of Absorbing Boundary Conditions

Let us consider that the smooth (closed) fictitious boundary $\Sigma := \partial\Omega$ is convex to ensure that the solution u is an outgoing wave to the computational domain Ω. We denote by s the anticlockwise directed curvilinear abscissa along Σ and by $\kappa := \kappa(s)$ the local (positive) curvature at s. If we introduce the curvilinear derivative ∂_s, then the Laplace-Beltrami operator over Σ is defined by $\Delta_\Sigma := \partial_s^2$.

To introduce properly the ABCs derived in [6], we need the fractional integration operators $I_t^{\alpha/2}$ of order $\alpha/2$ defined by

$$I_t^{\alpha/2} f(t) = \frac{1}{\Gamma(\alpha/2)} \int_0^t (t-s)^{\alpha/2-1} f(s)\, ds, \quad \text{for } \alpha \in \mathbb{N}. \tag{3}$$

where Γ designates the Gamma special function. Another operator is the fractional differential operator $\partial_t^{1/2}$ given by

$$\partial_t^{1/2} f(t) = \frac{1}{\sqrt{\pi}}\, \partial_t \int_0^t \frac{f(s)}{\sqrt{t-s}}\, ds. \tag{4}$$

The construction of the four families of absorbing boundary conditions (ABC) obtained in [6] was realized thanks to pseudodifferential operators theory and associated symbolic calculus. We refer to [6] for some notions about this theory. The symbols of the ABCs involve the curvilinear abscissa s, the time variable t but also their respective co-variable ξ and τ. Their derivation is restricted by the high frequency microlocal assumption which requires that the points (s, t, ξ, τ) lie in the quasi hyperbolic zone $\mathcal{H} = \{(s, t, \xi, \tau), -\tau - \xi^2 > 0\}$. As we will see later, we will need this assumption at the discrete level to guarantee good properties of the numerical schemes used to approximate system (1). The development of the different ABCs can be done following two strategies to which, once again, two kinds of approximations are associated. We therefore obtain four families of boundary conditions.

A first strategy is the following. Let us consider that u is the exact solution of system (1) and let us define $\mathcal{V}$ as a primitive of the potential V with respect to the time t

$$\mathcal{V}(x, y, t) = \int_0^t V(x, y, s)\, ds. \tag{5}$$

Let us introduce v as the new unknown defined by

$$v(x, y, t) = e^{-i\mathcal{V}(x,y,t)} u(x, y, t). \tag{6}$$

We obviously have $v_0(x, y) = u_0(x, y)$. Moreover, plugging u given by (5)–(6) into the Schrödinger equation with potential in (1) shows that v is solution to the variable coefficients Schrödinger equation

$$i\partial_t v + \Delta v + 2i\nabla\mathcal{V} \cdot \nabla v + \left(i\Delta\mathcal{V} - |\nabla\mathcal{V}|^2\right) v = 0, \quad \text{in } \Omega_T. \tag{7}$$

The fundamental reason why considering this change of unknown is crucial is that this first step would lead, in the one-dimensional case, to the Transparent Boundary Condition applied to v and associated to (7) for a time-dependent but x-independent potential. This is not the case if we work directly with the initial unknown u for (1) which would give an approximate artificial boundary condition even for a time-dependent and x-independent potential. We call this strategy the "Phase Function Transformation Strategy".

The second strategy, probably more natural, consists in building an approximate boundary condition based on the equation (1) with unknown u. We call this second strategy "Direct Strategy".

In each case, ABCs are obtained through a truncation of the asymptotic expansion of the total symbol of the Dirichlet-to-Neumann map. We thus obtain a sequence of ABCs of increasing order M, the integer M being the number of finite symbols considered in the asymptotic of the total symbol. This is what we call "a family of ABCs". It is expected that increasing M numerically improves the accuracy of the ABC.

The ABCs obtained by strategies I and II are nonlocal both in space and time. We propose two different techniques to build local versions of the ABCs. The first one, based on a high frequency hypothesis, is based on a Taylor expansion. However, it only gives access to local ABCs in space that however remain nonlocal in time. The second approach consists in considering approximations of ABCs at the symbolic level. We use in this case rational approximation (Padé approximation here) of the square-root. The advantage of this method is that it allows us to build fully local ABCs in space and time.

2.1. Strategy I: Phase Function Transformation

In strategy I and using a Taylor expansion to localize the boundary conditions with respect to time, the ABCs of order M are given by

$$\partial_{\mathbf{n}} u + \Lambda_{1,T}^{M} u = 0, \qquad \text{on } \Sigma_T, \tag{8}$$

where the operators $\Lambda_{1,T}^{M}$ are defined on Σ_T by

$$\Lambda_{1,T}^{2} u = e^{-i\pi/4} e^{i\mathcal{V}} \partial_t^{1/2} \left(e^{-i\mathcal{V}} u\right) + \frac{\kappa}{2} u, \tag{9}$$

$$\Lambda_{1,T}^{3} u = \Lambda_{1,T}^{2} u \tag{10}$$

$$-e^{i\pi/4} e^{i\mathcal{V}} \left(\frac{\kappa^2}{8} + \frac{\Delta_\Sigma}{2} + i\partial_s \mathcal{V} \partial_s + \frac{1}{2}(i\partial_s^2 \mathcal{V} - (\partial_s \mathcal{V})^2) \right) I_t^{1/2} \left(e^{-i\mathcal{V}} u\right), \tag{11}$$

$$\begin{aligned} \Lambda_{1,T}^{4} u = \Lambda_{1,T}^{3} u &+ i e^{i\mathcal{V}} \left(\frac{\partial_s(\kappa \partial_s)}{2} + \frac{\kappa^3 + \partial_s^2 \kappa}{8} + \frac{i\partial_s \kappa \partial_s \mathcal{V}}{2} \right) I_t \left(e^{-i\mathcal{V}} u\right) \\ &- i \frac{\mathrm{sg}(\partial_{\mathbf{n}} V)}{4} \sqrt{|\partial_{\mathbf{n}} V|}\, e^{i\mathcal{V}} I_t \left(\sqrt{|\partial_{\mathbf{n}} V|}\, e^{-i\mathcal{V}} u \right), \end{aligned} \tag{12}$$

and where the phase function $\mathcal{V}$ is given by

$$\mathcal{V}(x, y, t) = \int_0^t V(x, y, \sigma)\, d\sigma.$$

These ABCs are denoted by $\mathrm{ABC}_{1,T}^{M}$ in the sequel.

The second type of boundary conditions is given by the following formulation

$$\partial_{\mathbf{n}} u + \Lambda_{1,P}^{M} u = 0, \qquad \text{on } \Sigma_T \tag{13}$$

where the operators $\Lambda_{1,P}^{M}$ are defined on Σ_T by

$$\Lambda_{1,P}^{1} u = -ie^{i\mathcal{V}} \sqrt{i\partial_t + \Delta_\Sigma} \left(e^{-i\mathcal{V}} u\right), \tag{14}$$

$$\Lambda_{1,P}^{2} u = \Lambda_{1,P}^{1} u + \frac{\kappa}{2} u + \partial_s \mathcal{V} e^{i\mathcal{V}} \partial_s \left(i\partial_t + \Delta_\Sigma\right)^{-1/2} \left(e^{-i\mathcal{V}} u\right) \tag{15}$$

$$- \frac{\kappa}{2} e^{i\mathcal{V}} \left(i\partial_t + \Delta_\Sigma\right)^{-1} \Delta_\Sigma \left(e^{-i\mathcal{V}} u\right). \tag{16}$$

We specify these boundary conditions by $\mathrm{ABC}_{1,P}^{M}$. The idea is then to approximate the operators $\sqrt{i\partial_t + \Delta_\Sigma + V}$ and $\left(i\partial_t + \Delta_\Sigma + V\right)^{-1}$ by differential operators which allow us to build local versions of the ABCs. This operation is realized with Padé approximants (see section 3.4). We will denote this method by Padé approach in the sequel.

2.2. Strategy II: direct method

In strategy II (direct method) and following Taylor expansions, the ABCs of order M are given by

$$\partial_{\mathbf{n}} u + \Lambda_{2,T}^{M} u = 0, \quad \text{on } \Sigma_T. \tag{17}$$

The operators $\Lambda_{2,T}^{M}$ are defined on Σ_T by

$$\Lambda_{2,T}^{1} u = e^{-i\pi/4} \partial_t^{1/2} u, \tag{18}$$

$$\Lambda_{2,T}^{2} u = \Lambda_{2,T}^{1} u + \frac{\kappa}{2} u, \tag{19}$$

$$\Lambda_{2,T}^{3} u = \Lambda_{2,T}^{2} u - e^{i\pi/4} \left(\frac{\kappa^2}{8} + \frac{\Delta_\Sigma}{2}\right) I_t^{1/2} u \tag{20}$$

$$- e^{i\pi/4} \frac{\mathrm{sg}(V)}{2} \sqrt{|V|}\, I_t^{1/2} \left(\sqrt{|V|}\, u\right),$$

$$\Lambda_{2,T}^{4} u = \Lambda_{2,T}^{3} u + i \left(\frac{\partial_s(\kappa \partial_s)}{2} + \frac{\kappa^3 + \partial_s^2 \kappa}{8}\right) I_t\, u \tag{21}$$

$$- i \frac{\mathrm{sg}(\partial_{\mathbf{n}} V)}{4} \sqrt{|\partial_{\mathbf{n}} V|}\, I_t \left(\sqrt{|\partial_{\mathbf{n}} V|}\, u\right).$$

The boundary conditions are denoted by $\mathrm{ABC}_{2,T}^{M}$ in the rest of the paper.

Following the Padé approach like in strategy I, the ABCs of order M are given by

$$\partial_{\mathbf{n}} u + \Lambda_{2,P}^{M} u = 0, \quad \text{on } \Sigma_T, \tag{22}$$

where the operators $\Lambda_{2,P}^M$ are defined on Σ_T by

$$\Lambda_{2,P}^1 u = -i\sqrt{i\partial_t + \Delta_\Sigma + V}\, u, \tag{23}$$

$$\Lambda_{2,P}^2 u = \Lambda_{2,P}^2 u + \frac{\kappa}{2}u - \frac{\kappa}{2}\left(i\partial_t + \Delta_\Sigma + V\right)^{-1}\Delta_\Sigma u. \tag{24}$$

The ABCs are denoted by $\mathrm{ABC}_{2,P}^M$.

Remark 2.1. *. The construction of the ABCs may be generalized to the case of nonlinear problems. The idea is to replace formally the potential by the nonlinearity in the above ABCs. Considering schemes adapted to nonlinear problems, some of the points described below can be used. The way the ABCs compare might be different from what we observe in the potential case, partly due to heavy computational costs for some of the ABCs. Some numerical results for a cubic nonlinearity are presented in [5] showing accurate results.*

3. Semi-discretization of the boundary conditions

We have obtained four families of artificial boundary conditions labelled $\mathrm{ABC}_{1,T}^M$, $\mathrm{ABC}_{1,P}^M$, $\mathrm{ABC}_{2,T}^M$ and $\mathrm{ABC}_{2,P}^M$, for different orders $M \in \{1,2,3,4\}$. The associated operators linked to these boundary conditions are given by the equations (8), (13), (17) and (22). The aim of this section is to present the semi-discrete (with respect to time) numerical schemes associated to these different absorbing boundary conditions. In a first step, we are interested in the semi-discretization of the equation in the computational domain Ω. The second step consists in studying the properties of the discretizations for each ABC.

3.1. Semi-discrete interior scheme

We have to deal with the following IBVP for the Schrödinger equation

$$\begin{cases} i\partial_t u + \Delta u + V\,u = 0, & \text{in } \Omega_T, \\ \partial_{\mathbf{n}} u + \Lambda^M u = 0, & \text{on } \Sigma_T, \\ u(\cdot,0) = u_0, & \text{in } \Omega, \end{cases} \tag{25}$$

where Λ^M denotes one of the operators of order M, $M \in \{1,2,3,4\}$, among the four families of ABCs. We set N as the number of time steps for a uniform discretization of $[0;T]$. Therefore, we have $\Delta t = T/N$. For $t_n = n\Delta t$, with $0 \le n \le N$, $u^n(\mathbf{x})$ designates an approximation of $u(\mathbf{x}, t_n)$. A semi-discrete approximation adapted to the Schrödinger equation on Ω_T is given by the Crank-Nicolson scheme

$$i\frac{u^{n+1} - u^n}{\Delta t} + \Delta\frac{u^{n+1} + u^n}{2} + \frac{V^{n+1} + V^n}{2}\frac{u^{n+1} + u^n}{2} = 0, \quad 0 \le n \le N, \tag{26}$$

setting $V^n = V(\mathbf{x}, t_n)$. For implementation issues, it is useful to introduce the new variables $v^{n+1} = u^{n+1/2} = \frac{u^{n+1}+u^n}{2}$ and $W^{n+1} = V^{n+1/2} = \frac{V^{n+1}+V^n}{2}$, with $v^0 = u^0$ and $W^0 = V^0$. The scheme can then be written

$$\frac{2i}{\Delta t}v^{n+1} + \Delta v^{n+1} + W^{n+1}v^{n+1} = \frac{2i}{\Delta t}u^n, \quad 0 \le n \le N. \tag{27}$$

It is well-known that a discretization of the ABC which preserves the stability of the Crank-Nicolson scheme for the free-potential Schrödinger equation is not a trivial task. We propose here two solutions for the discretization of $\mathrm{ABC}^M_{\cdot,\{T,P\}}$. The first one is based on semi-discretization of the fractional operators involved in (8) and (13). We are then able to show that the resulting semi-discrete scheme is unconditionally stable. At the same time, a solution based on convolution operators may require long computational times (but can be strongly accelerated through recent fast algorithms [25]). The second solution that we study is based on the approximation of the fractional operators through the solution of auxiliary time-dependent partial differential equations on Σ. The evaluation is then extremely efficient but at the same time no stability proof is available.

In a first step, we study the discretization of the boundary conditions $\mathrm{ABC}^M_{1,T}$ and $\mathrm{ABC}^M_{2,T}$ based on a Taylor expansion. Next, we will consider the discretization of the boundary conditions $\mathrm{ABC}^M_{1,P}$ and $\mathrm{ABC}^M_{2,P}$ related to Padé approximants.

3.2. Discretization of the boundary conditions $ABC^M_{1,T}$ and $ABC^M_{2,T}$

The boundary conditions $\mathrm{ABC}^M_{\cdot,T}$ involve fractional derivatives and integral operators which are discretized by using discrete convolutions of the operators $\partial_t^{1/2}$, $I_t^{1/2}$ and I_t [3, 4, 7]. If $\{f^n\}_{n\in\mathbb{N}}$ is a sequence of complex numbers approximating $\{f(t_n)\}_{n\in\mathbb{N}}$, then the approximations of $\partial_t^{1/2}f(t_n)$, $I_t^{1/2}f(t_n)$ and $I_t\,f(t_n)$ with respect to the Crank-Nicolson scheme for a time step Δt are given by the numerical quadrature formulas

$$\partial_t^{1/2}f(t_n) \approx \sqrt{\frac{2}{\Delta t}}\sum_{k=0}^{n}\beta_{n-k}f^k = \sqrt{\frac{2}{\Delta t}}(\beta_k \star f^k)_n, \tag{28}$$

$$I_t^{1/2}f(t_n) \approx \sqrt{\frac{\Delta t}{2}}\sum_{k=0}^{n}\alpha_{n-k}f^k = \sqrt{\frac{\Delta t}{2}}(\alpha_k \star f^k)_n, \tag{29}$$

$$I_t\,f(t_n) \approx \frac{\Delta t}{2}\sum_{k=0}^{n}\gamma_{n-k}f^k = \frac{\Delta t}{2}(\gamma_k \star f^k)_n, \tag{30}$$

where the sequences $(\alpha_n)_{n\in\mathbb{N}}$, $(\beta_n)_{n\in\mathbb{N}}$ and $(\gamma_n)_{n\in\mathbb{N}}$ are

$$\begin{cases} (\alpha_0,\alpha_1,\alpha_2,\alpha_3,\alpha_4,\alpha_5,\ldots) = (1,1,\frac{1}{2},\frac{1}{2},\frac{3}{8},\frac{3}{8},\ldots), \\ \beta_k = (-1)^k\alpha_k, \quad \forall k\geq 0, \\ (\gamma_0,\gamma_1,\gamma_2,\gamma_3,\ldots) = (1,2,2,2,\ldots). \end{cases} \tag{31}$$

We denote by b^{n+1} the convolution product $(\beta_k\star v^k)_{n+1}$, also written $\beta_{n+1}\star v^{n+1}$.

Proposition 3.1. *The semi-discrete Crank-Nicolson scheme for* (25) *with bound-*

ary conditions $ABC_{2,T}^M$ *is given by*

$$\begin{cases} \dfrac{2i}{\Delta t} v^{n+1} + \Delta v^{n+1} + W^{n+1}\, v^{n+1} = \dfrac{2i}{\Delta t} u^n, \quad \textit{on } \Omega, \\ \partial_{\mathbf{n}} v^{n+1} + \Lambda_{2,T}^{M,n+1} v^{n+1} = 0, \quad \textit{on } \Sigma, \\ u^0 = u_0, \quad \textit{on } \Omega, \end{cases} \tag{32}$$

for $n = 0, \ldots, N-1$*. The semi-discrete operators* $\Lambda_{2,T}^{M,n+1}$*,* $M \in \{1,2,3,4\}$*, are given by*

$$\Lambda_{2,T}^{1,n+1} v^{n+1} = e^{-i\pi/4} \sqrt{\frac{2}{\Delta t}} b^{n+1}, \tag{33}$$

$$\Lambda_{2,T}^{2,n+1} v^{n+1} = \Lambda_{2,T}^{1,n+1} v^{n+1} + \frac{\kappa}{2} v^{n+1}, \tag{34}$$

$$\begin{aligned} \Lambda_{2,T}^{3,n+1} v^{n+1} &= \Lambda_{2,T}^{2,n+1} v^{n+1} \\ &- e^{i\pi/4} \sqrt{\frac{\Delta t}{2}} \left(\frac{\kappa^2}{8} a_0^{n+1} + \frac{1}{2} a_2^{n+1} + \frac{1}{2} \operatorname{sg}(W^{n+1}) \sqrt{|W^{n+1}|}\, a_V^{n+1} \right), \end{aligned} \tag{35}$$

$$\begin{aligned} \Lambda_{2,T}^{4,n+1} v^{n+1} = \Lambda_{2,T}^{3,n+1} v^{n+1} + i \frac{\Delta t}{2} \Bigg(\frac{1}{2} \partial_s (\kappa d_1^{n+1}) + \frac{\kappa^3 + \partial_s^2 \kappa}{8} d_0^{n+1} \\ - \frac{1}{4} \operatorname{sg}(\partial_{\mathbf{n}} W^{n+1}) \sqrt{|\partial_{\mathbf{n}} W^{n+1}|}\, d_V^{n+1} \Bigg), \end{aligned} \tag{36}$$

with the following notations

$$b^{n+1} = \left(\beta_k \star v^k\right)_{n+1}, \tag{37}$$

$$a_\mu^{n+1} = \left(\alpha_k \star \left(\partial_s^\mu v^k\right)\right)_{n+1}, \quad \mu \in \{0,1,2\}, \tag{38}$$

$$a_V^{n+1} = \left(\alpha_k \star \left(\sqrt{|W^k|}\, v^k\right)\right)_{n+1}, \tag{39}$$

$$d_\mu^{n+1} = \left(\gamma_k \star \left(\partial_s^\mu v^k\right)\right)_{n+1}, \quad \mu \in \{0,1\}, \tag{40}$$

$$d_V^{n+1} = \left(\gamma_k \star \left(\sqrt{|\partial_{\mathbf{n}} W^k|}\, v^k\right)\right)_{n+1}. \tag{41}$$

In order to build a discretization of $\mathrm{ABC}_{1,T}^M$, we have to consider the various terms coming from the phase function transformation and to approximate the phase function $\mathcal{V}$ by

$$\mathscr{W}^{n+1} = \mathcal{V}^{n+1/2} = \frac{\mathcal{V}^{n+1} + \mathcal{V}^n}{2}.$$

Proposition 3.2. *The semi-discrete Crank-Nicolson scheme for* (25) *with boundary conditions* $ABC_{1,T}^M$ *is given by*

$$\begin{cases} \dfrac{2i}{\Delta t} v^{n+1} + \Delta v^{n+1} + W^{n+1} v^{n+1} = \dfrac{2i}{\Delta t} u^n, \quad \textit{on } \Omega, \\ \partial_{\mathbf{n}} v^{n+1} + \Lambda_{1,T}^{M,n+1} v^{n+1} = 0, \quad \textit{on } \Sigma, \\ u^0 = u_0, \quad \textit{on } \Omega, \end{cases} \tag{42}$$

for $n = 0, \ldots, N-1$, where the semi-discrete operators $\Lambda_{1,T}^{M,n+1}$, $M \in \{2,3,4\}$, are given by

$$\Lambda_{1,T}^{2,n+1} v^{n+1} = e^{-i\pi/4} \sqrt{\frac{2}{\Delta t}} e^{i\mathscr{W}^{n+1}} \widetilde{b}^{n+1} + \frac{\kappa}{2} v^{n+1}, \tag{43}$$

$$\begin{aligned}\Lambda_{1,T}^{3,n+1} v^{n+1} = \Lambda_{1,T}^{2,n+1} v^{n+1} - e^{i\pi/4} \sqrt{\frac{\Delta t}{2}} \Bigg(& \frac{\kappa^2}{8} e^{i\mathscr{W}^{n+1}} \widetilde{a}_0^{n+1} \\ & + \frac{1}{2} e^{i\mathscr{W}^{n+1}} \widetilde{a}_2^{n+1} + i(\partial_s \mathscr{W}^{n+1}) e^{i\mathscr{W}^{n+1}} \widetilde{a}_1^{n+1} \\ & + \frac{1}{2} \left(i\partial_s^2 \mathscr{W}^{n+1} - (\partial_s \mathscr{W}^{n+1})^2 \right) e^{i\mathscr{W}^{n+1}} \widetilde{a}_0^{n+1} \Bigg),\end{aligned} \tag{44}$$

$$\begin{aligned}\Lambda_{1,T}^{4,n+1} v^{n+1} = \Lambda_{1,T}^{3,n+1} v^{n+1} + i \Bigg(& \frac{1}{2} e^{i\mathscr{W}^{n+1}} \partial_s (\kappa \widetilde{d}_1^{n+1}) \\ & + \frac{\kappa^3 + \partial_s^2 \kappa}{8} e^{i\mathscr{W}^{n+1}} \widetilde{d}_0^{n+1} + \frac{i}{2} (\partial_s \kappa)(\partial_s \mathscr{W}^{n+1}) e^{i\mathscr{W}^{n+1}} \widetilde{d}_0^{n+1} \\ & - \frac{i}{4} \operatorname{sg}(\partial_{\mathbf{n}} W^{n+1}) \sqrt{|\partial_{\mathbf{n}} W^{n+1}|} \, e^{i\mathscr{W}^{n+1}} \widetilde{d}_V^{n+1} \Bigg).\end{aligned} \tag{45}$$

In the above notations, we have set

$$\widetilde{b}^{n+1} = \left(\beta_k \star \left(e^{-i\mathscr{W}^k} v^k \right) \right)_{n+1}, \tag{46}$$

$$\widetilde{a}_\mu^{n+1} = \left(\alpha_k \star \left(\partial_s^\mu \left(e^{-i\mathscr{W}^k} v^k \right) \right) \right)_{n+1}, \quad \mu \in \{0,1,2\}, \tag{47}$$

$$\widetilde{d}_\mu^{n+1} = \left(\gamma_k \star \left(\partial_s^\mu \left(e^{-i\mathscr{W}^k} v^k \right) \right) \right)_{n+1}, \quad \mu \in \{0,1\}, \tag{48}$$

$$\widetilde{d}_V^{n+1} = \left(\gamma_k \star \left(e^{-i\mathscr{W}^k} \sqrt{|\partial_{\mathbf{n}} W^k|} \, v^k \right) \right)_{n+1}. \tag{49}$$

Remark 3.1. . *In the case of radially symetrical potential $V = V(r,t)$ and domain Ω, the operators $\Lambda_{1,T}^{3,n+1}$ and $\Lambda_{1,T}^{4,n+1}$ have a simplified form*

$$\begin{aligned}\Lambda_{1,T}^{3,n+1} v^{n+1} = \Lambda_{1,T}^{2,n+1} v^{n+1} - e^{i\pi/4} \sqrt{\frac{\Delta t}{2}} \Bigg(& \frac{\kappa^2}{8} e^{i\mathscr{W}^{n+1}} \widetilde{a}_0^{n+1} \\ & + \frac{1}{2} e^{i\mathscr{W}^{n+1}} \widetilde{a}_2^{n+1} \Bigg),\end{aligned} \tag{50}$$

$$\begin{aligned}\Lambda_{1,T}^{4,n+1} v^{n+1} = {} & \Lambda_{1,T}^{3,n+1} v^{n+1} + i \Bigg(\frac{1}{2} e^{i\mathscr{W}^{n+1}} \partial_s (\kappa \widetilde{d}_1^{n+1}) \\ & + \frac{\kappa^3 + \partial_s^2 \kappa}{8} e^{i\mathscr{W}^{n+1}} \widetilde{d}_0^{n+1} - \frac{i}{4} \operatorname{sg}(\partial_{\mathbf{n}} W^{n+1}) \sqrt{|\partial_{\mathbf{n}} W^{n+1}|} \, e^{i\mathscr{W}^{n+1}} \widetilde{d}_V^{n+1} \Bigg),\end{aligned} \tag{51}$$

with the modified coefficients $\widetilde{a}_\mu^{n+1}$ *and* $\widetilde{d}_\mu^{n+1}$

$$\widetilde{b}_\mu^{n+1} = \left(\alpha_k \star \left(e^{-i\mathscr{W}^k}\partial_s^\mu v^k\right)\right)_{n+1}, \quad \mu \in \{0,1,2\}, \tag{52}$$

$$\widetilde{d}_\mu^{n+1} = \left(\gamma_k \star \left(e^{-i\mathscr{W}^k}\partial_s^\mu v^k\right)\right)_{n+1}, \quad \mu \in \{0,1\}, \tag{53}$$

since $\partial_s \mathscr{W}^{n+1} = 0$.

3.3. *Stability results for the Crank-Nicolson scheme associated with the discretized boundary conditions* $ABC_{1,T}^M$ *and* $ABC_{2,T}^M$

We derive in this section *a priori* estimates for the systems (32) and (42). To prove these results, it is necessary to recall that the ABCs are obtained through symbolic calculus linked to underlying pseudodifferential operators. As already said, their validity requires a condition in the quasi hyperbolic zone $\mathcal{H}$. This condition is nothing but a relation on the positivity of the real part of the symbol $\sigma(P_\Sigma)$ of the Schrödinger operator on the boundary

$$P_\Sigma : f \mapsto P_\Sigma(f) = i\partial_t f + \Delta_\Sigma f.$$

It is obtained by

$$\mathscr{F}_{(s,t)}\left(P_\Sigma(f)\right) = \sigma(P_\Sigma)\mathscr{F}_{(s,t)}(f),$$

where $\sigma(P_\Sigma) = -\tau - \xi^2$ and $\mathscr{F}_{(s,t)}$ denotes the Fourier transform with respect to the variables s and t. The restriction to the quasi hyperbolic zone $\mathcal{H}$ also reads: $\mathrm{Re}(-\tau-\xi^2) > 0$ and $\mathrm{Im}(-\tau-\xi^2) = 0$. This definition is only available in the continuous framework. In the discrete case, we have to adapt this definition to the Crank-Nicolson scheme.

The semi-discrete operator $\widetilde{P_\Sigma}$ associated with P_Σ and linked to the Crank-Nicolson scheme is

$$\widetilde{P_\Sigma} : f \mapsto \left(i\frac{f(t_{n+1}) - f(t_n)}{\Delta t} + \Delta_\Sigma \frac{f(t_{n+1}) + f(t_n)}{2}\right)_{n\in\mathbb{N}}.$$

We identify its associated symbol replacing the Fourier transform used in the continuous framework by the $\mathcal{Z}$-transform (see Annex A)

$$\mathscr{F}_s\mathcal{Z}\left(\widetilde{P_\Sigma}(f)\right) = \sigma_{\mathrm{sd}}(\widetilde{P_\Sigma})\mathscr{F}_s\mathcal{Z}(f(t_n))(z),$$

with

$$\sigma_{\mathrm{sd}}\left(\widetilde{P_\Sigma}\right) = \frac{i}{\Delta t}(z-1) - \frac{\xi^2}{2}(z+1) = \frac{z+1}{2}\left(\frac{2i}{\Delta t}\frac{z-1}{z+1} - \xi^2\right). \tag{54}$$

The property that the quadruplet (s,t,ξ,τ) belongs to the quasi hyperbolic zone $\mathcal{H}$ is: $-\tau-\xi^2 > 0$, which means that $\mathrm{Re}\left(\sigma(P_\Sigma)\right) > 0$ and $\mathrm{Im}\left(\sigma(P_\Sigma)\right) = 0$. Similarly, we define the semi-discrete quasi hyperbolic zone, denoted by $\mathcal{H}_{\mathrm{sd}}$, whose characterization is linked to the semi-discrete symbol of $\widetilde{P_\Sigma}$.

Definition 3.1. *The semi-discrete quasi hyperbolic zone $\mathcal{H}_{sd}$ is the set of quadruplets $(s, n, \xi, z) \in \mathbb{R} \times \mathbb{N} \times \mathbb{R} \times \mathbb{C}$ satisfying*

$$\mathrm{Re}\left(\frac{2i}{\Delta t}\frac{z-1}{z+1} - \xi^2\right) > 0 \quad \textit{and} \quad \mathrm{Im}\left(\frac{2i}{\Delta t}\frac{z-1}{z+1} - \xi^2\right) = 0.$$

Therefore, the characterization $\sigma(P_\Sigma) \in \mathbb{R}^{+*}$ is transposed to the semi-discrete domain as $\frac{2i}{\Delta t}\frac{z-1}{z+1} - \xi^2 \in \mathbb{R}^{+*}$.

Let us begin with the approximation of the boundary condition $\mathrm{ABC}_{2,T}^{M}$. We have the following result:

Theorem 3.1. *Let $(u^n)_{0\leq n \leq N}$ be a solution of the system*

$$\begin{cases} i\,\dfrac{u^{n+1}-u^n}{\Delta t} + \Delta v^{n+1} + W^{n+1}\, v^{n+1} = 0, \quad \textit{in } \Omega, \\ \partial_{\mathbf{n}} v^{n+1} + \Lambda_{2,T}^{M,n+1} v^{n+1} = 0, \qquad \textit{on } \Sigma, \quad \textit{for } M \in \{2,3,4\}, \\ u^0 = u_0, \quad \textit{in } \Omega. \end{cases} \tag{55}$$

For $M = 2$, we have the following energy inequality

$$\forall n \in \{0, \ldots, N\}, \quad \|u^n\|_{L^2(\Omega)} \leq \|u^0\|_{L^2(\Omega)}. \tag{56}$$

Moreover, if $\mathrm{sg}(W^k) = 1$ on Σ for any time t_k, then the inequality (56) remains satisfied for $M = 3$. In addition, if $\kappa > 0$, $\kappa^3 + \partial_s^2 \kappa < 0$ and $\mathrm{sg}(\partial_{\mathbf{n}} W^k) = 1$ on Σ, then this inequality is also satisfied for $M = 4$.

Remark 3.2. . *We only state uniqueness results in Theorem 3.1. Existence should be also studied to get a complete Theorem.*

Proof. A classical algebraic manipulation leads to the identity

$$\frac{\|u^P\|^2_{L^2(\Omega)} - \|u^0\|^2_{L^2(\Omega)}}{2\Delta t} = \mathrm{Re}\left(\sum_{n=0}^{P-1} \int_\Sigma i\overline{v^{n+1}}\partial_{\mathbf{n}} v^{n+1} d\Sigma\right) = \mathrm{Re}\left(\sum_{n=0}^{P-1} A^n\right), \tag{57}$$

where A^n denotes the term $\int_\Sigma i\overline{v^{n+1}}\partial_{\mathbf{n}} v^{n+1} d\Sigma$.

To prove (56), one needs to show that the right hand side of (57) is negative. Since $\mathrm{sg}(W^{n+1}) = \mathrm{sg}(\partial_{\mathbf{n}} W^{n+1}) = 1$ on Σ for all times t_{n+1} and v^0 has compact support in Ω, a simple computation allows us to write

$$\begin{aligned}
\sum_{n=0}^{P-1}\int_\Sigma i\overline{v^{n+1}}\partial_{\mathbf{n}}v^{n+1}d\Sigma = &-e^{i\pi/4}\sqrt{\frac{1}{2\Delta t}}\int_\Sigma\sum_{n=0}^{P}b^n\overline{v^n}d\Sigma\\
&-\frac{i}{2}\int_\Sigma\kappa\sum_{n=0}^{P}|v^n|^2\,d\Sigma\\
&+ie^{i\pi/4}\sqrt{\frac{\Delta t}{2}}\int_\Sigma\sum_{n=0}^{P}\left(\frac{i}{\Delta t}b^n\overline{v^n}+\frac{1}{2}a_0^n\,\overline{\partial_s^2 v^n}\right)d\Sigma\\
&+ie^{i\pi/4}\sqrt{\frac{\Delta t}{2}}\int_\Sigma\frac{\kappa^2}{8}\sum_{n=0}^{P}a_0^n\overline{v^n}d\Sigma\\
&+ie^{i\pi/4}\sqrt{\frac{\Delta t}{2}}\int_\Sigma\frac{1}{2}\sum_{n=0}^{P}a_V^n\sqrt{|W^n|}\,\overline{v^n}d\Sigma\\
&-\frac{\Delta t}{2}\int_\Sigma\frac{\kappa}{2}\sum_{n=0}^{P}d_1^n\partial_s\overline{v^n}d\Sigma\\
&+\frac{\Delta t}{2}\int_\Sigma\frac{\kappa^3+\Delta_\kappa}{8}\sum_{n=0}^{P}d_0^n\overline{v^n}d\Sigma\\
&-\frac{\Delta t}{2}\int_\Sigma\frac{1}{4}\,\mathrm{sg}(\partial_{\mathbf{n}}W^0)\sum_{n=0}^{P}d_V^n\sqrt{|\partial_{\mathbf{n}}W^n|}\,\overline{v^n}d\Sigma.
\end{aligned}\tag{58}$$

The proof mainly relies on Lemmas A.1 and A.2 (see Annex A). Let us apply them to the first term of the right hand side of (58). One has

$$Q_\beta := \sum_{n=0}^{P}\overline{v^n}b^n = \sum_{n=0}^{P}\left(\overline{v^n}\sum_{k=0}^{n}\beta_{n-k}v^k\right) = \sum_{n=0}^{P}\overline{v^n}(\beta_n\star v^n).$$

Thanks to Lemma A.2, $-e^{i\pi/4}Q_\beta$ has a negative real part. The study of the other terms is quite similar except for the third one for which the proof is more delicate. We study the real part of the quantity

$$B_3 = ie^{i\pi/4}\sqrt{\frac{\Delta t}{2}}\int_\Sigma\sum_{n=0}^{P}\left(\frac{i}{\Delta t}b^n\overline{v^n}+\frac{1}{2}a_0^n\,\overline{\partial_s^2 v^n}\right)d\Sigma.$$

Using the Plancherel's theorem for the Fourier transform along the curvilinear abscissa s (with covariable ξ), we get

$$B_3 = ie^{i\pi/4}\sqrt{\frac{\Delta t}{2}}\int_{\mathbb{R}}\sum_{n=0}^{P}\left(\frac{i}{\Delta t}\widehat{b^n}\,\overline{\widehat{v^n}}-\frac{\xi^2}{2}\widehat{a_0^n}\,\overline{\widehat{v^n}}\right)d\xi.$$

By using Lemma A.1 (see Annex A), we have

$$B_3 = ie^{i\pi/4}\sqrt{\frac{\Delta t}{2}}\int_{\mathbb{R}}\frac{1}{2\pi}\int_{-\pi}^{\pi}\left[\frac{i}{\Delta t}\hat{\beta}(e^{i\omega}) - \frac{\xi^2}{2}\hat{\alpha}(e^{i\omega})\right]\left|\sum_{n=0}^{P}\widehat{v^n}e^{-i\omega n}\right|^2 d\omega,$$

which reduces to

$$B_3 = ie^{i\pi/4}\sqrt{\frac{\Delta t}{2}}\int_{\mathbb{R}}\frac{1}{2\pi}\int_{-\pi}^{\pi}\left[\frac{i}{\Delta t}\sqrt{\frac{e^{i\omega}-1}{e^{i\omega}+1}} - \frac{\xi^2}{2}\sqrt{\frac{e^{i\omega}+1}{e^{i\omega}-1}}\right]\cdot \left|\sum_{n=0}^{P}\widehat{v^n}e^{-i\omega n}\right|^2 d\omega. \quad (59)$$

The study of the sign of the real part of B_3 is thus reduced to the study of the sign of the real part of the complex function $R(z)$ defined by

$$R(z) = ie^{i\pi/4}\left(\frac{i}{\Delta t}\sqrt{\frac{z-1}{z+1}} - \frac{\xi^2}{2}\sqrt{\frac{z+1}{z-1}}\right) \quad (60)$$

on the unit circle. Another equivalent form is

$$R(z) = \frac{i}{2}e^{i\pi/4}\sqrt{\frac{z+1}{z-1}}\left(\frac{2i}{\Delta t}\frac{z-1}{z+1} - \xi^2\right). \quad (61)$$

Therefore, the function $R(z)$ can be written as

$$R(z) = \sigma(z)\left(\frac{2i}{\Delta t}\frac{z-1}{z+1} - \xi^2\right),$$

where σ is the function defined by

$$\sigma(z) = \frac{i}{2}e^{i\pi/4}\sqrt{\frac{z+1}{z-1}}.$$

Since we are working in the semi-discrete quasi hyperbolic zone $\mathcal{H}_{\rm sd}$, we have $\frac{2i}{\Delta t}\frac{z-1}{z+1} - \xi^2 > 0$. The problem is therefore reduced to the study of the real part of the function σ on the unit circle. But for $\omega \in (-\pi;\pi)$, one has $\sqrt{\frac{e^{i\omega}+1}{e^{i\omega}-1}} = \sqrt{-i\,\mathrm{cotan}\left(\frac{\omega}{2}\right)}$. Hence, the application $z \mapsto \sqrt{\frac{z+1}{z-1}}$ maps the unit circle onto $e^{-i\pi/4}\mathbb{R}^+ \cup e^{i\pi/4}\mathbb{R}^+$. Thus, we have that $\mathrm{Re}\left(\sigma(z)\right) \leq 0$ when $z = e^{i\omega}$ belongs to the unit circle. This proves that the term B_3 given by (59) has a negative real part. □

For the boundary conditions obtained by the Phase Function Transformation, we have an equivalent theorem but under stronger hypothesis on the potential and the computational domain.

Theorem 3.2. *Let $(u^n)_{0\le n\le N}$ be a solution of the system*

$$\begin{cases} i\,\dfrac{u^{n+1}-u^n}{\Delta t} + \Delta v^{n+1} + W^{n+1}\,v^{n+1} = 0, \quad \text{in } \Omega, \\ \partial_{\mathbf{n}} v^{n+1} + \Lambda_{1,T}^{M,n+1} v^{n+1} = 0, \quad \text{on } \Sigma, \quad \text{for } M \in \{2,3,4\}, \\ u^0 = u_0, \quad \text{in } \Omega. \end{cases} \tag{62}$$

For $M = 2$, we have the following energy inequality

$$\forall n \in \{0,\dots,N\}, \quad \|u^n\|_{L^2(\Omega)} \le \|u^0\|_{L^2(\Omega)}. \tag{63}$$

Moreover, if the potential V and the computational domain Ω are radially symetrical, then the inequality (56) *remains satisfied for $M = 3$. Finally, if* $\mathrm{sg}(\partial_{\mathbf{n}} W^k)$ *is time independent on Σ, then this inequality is also satisfied for $M = 4$.*

We omit the proof which is similar to the previous one. We refer to [16] for more details.

Remark 3.3. . *Let us point out here that the stability results in Theorems 3.1 and 3.2 exactly correspond to well-posedness results obtained in [6] at the continuous level under the same kind of assumptions.*

3.4. Discretization of the boundary conditions $ABC_{1,P}^M$ and $ABC_{2,P}^M$

An alternative approach to discrete convolutions consists in approximating the square-root operator $\sqrt{i\partial_t + V}$ by using rational functions and more precisely using the m-th order Padé approximants [22]

$$\sqrt{z} \approx R_m(z) = a_0^m + \sum_{k=1}^{m} \frac{a_k^m\, z}{z + d_k^m} = \sum_{k=0}^{m} a_k^m - \sum_{k=1}^{m} \frac{a_k^m\, d_k^m}{z + d_k^m}, \tag{64}$$

where the coefficients $(a_k^m)_{0\le k\le m}$ and $(d_k^m)_{1\le k\le m}$ are given by

$$a_0^m = 0 \quad , \quad a_k^m = \frac{1}{m\cos^2\left(\frac{(2k+1)\pi}{4m}\right)} \quad , \quad d_k^m = \tan^2\left(\frac{(2k+1)\pi}{4m}\right). \tag{65}$$

Formally, $\sqrt{i\partial_t + V}$ is approximated by

$$R_m(i\partial_t + V) = \sum_{k=0}^{m} a_k^m - \sum_{k=1}^{m} a_k^m\, d_k^m (i\partial_t + V + d_k^m)^{-1}. \tag{66}$$

Let us begin by applying this technique to the absorbing boundary conditions $\mathrm{ABC}_{2,P}^M$ coming from the direct strategy

$$\partial_{\mathbf{n}} u - i\sqrt{i\partial_t + \Delta_\Sigma + V}\, u + \frac{\kappa}{2} u - \frac{\kappa}{2}\left(i\partial_t + \Delta_\Sigma + V\right)^{-1} \Delta_\Sigma u = 0, \quad \text{on } \Sigma.$$

By using (66), we get

$$\partial_{\mathbf{n}} u - i\sum_{k=0}^{m} a_k^m u + i\sum_{k=1}^{m} a_k^m d_k^m \left(i\partial_t + \Delta_\Sigma + V + d_k^m\right)^{-1} u + \frac{\kappa}{2}u \\ - \frac{\kappa}{2}\left(i\partial_t + \Delta_\Sigma + V\right)^{-1}\Delta_\Sigma u = 0.$$

To write a suitable form of the equation in view of an efficient numerical treatment, we classically introduce $m+1$ auxiliary functions φ_k, for $1 \leq k \leq m$, and ψ (see Lindmann [21]) as follows

$$\varphi_k = \left(i\partial_t + \Delta_\Sigma + V + d_k^m\right)^{-1} u,$$

and

$$\psi = \left(i\partial_t + \Delta_\Sigma + V\right)^{-1}\Delta_\Sigma u.$$

The corresponding full absorbing boundary condition is written as a system associated to the condition $\mathrm{ABC}_{2,P}^2$

$$\begin{cases} \partial_{\mathbf{n}} u - i\sum_{k=0}^{m} a_k^m u + i\sum_{k=1}^{m} a_k^m d_k^m \varphi_k + \frac{\kappa}{2}u - \frac{\kappa}{2}\psi = 0, \quad \text{on } \Sigma_T, \\ i\partial_t\varphi_k + \Delta_\Sigma\varphi_k + V\varphi_k + d_k^m\varphi_k = u, \quad \text{on } \Sigma_T, \quad \text{for } 1 \leq k \leq m, \\ i\partial_t\psi + \Delta_\Sigma\psi + V\psi = \Delta_\Sigma u, \quad \text{on } \Sigma_T, \\ \varphi_k(\mathbf{x},0) = 0,\ 1 \leq k \leq m, \quad \psi(\mathbf{x},0) = 0, \quad \text{for } \mathbf{x} \in \Sigma. \end{cases} \tag{67}$$

Now, we have to discretize the above system. The semi-discretization of the interior scheme remains the same as before (see Eq. (27)) and consequently (67) becomes for $0 \leq n \leq N$

$$\begin{cases} \partial_{\mathbf{n}} v^{n+1} - i\sum_{k=0}^{m} a_k^m v^{n+1} + \frac{\kappa}{2}v^{n+1} + i\sum_{k=1}^{m} a_k^m d_k^m \varphi_k^{n+1/2} - \frac{\kappa}{2}\psi^{n+1/2} = 0, \\ \left(\frac{2i}{\Delta t} + \Delta_\Sigma + W^{n+1} + d_k^m\right)\varphi_k^{n+1/2} - v^{n+1} = \frac{2i}{\Delta t}\varphi_k^n, \quad 1 \leq k \leq m, \\ \left(\frac{2i}{\Delta t} + \Delta_\Sigma + W^{n+1}\right)\psi^{n+1/2} - \Delta_\Sigma v^{n+1} = \frac{2i}{\Delta t}\psi^n, \\ \varphi_k(\mathbf{x},0) = 0 \quad \text{for } 1 \leq k \leq m, \quad \psi^0(\mathbf{x}) = 0 \quad \text{on } \Sigma, \end{cases} \tag{68}$$

where $\varphi_k^{n+1/2} = \frac{\varphi_k^{n+1} + \varphi_k^n}{2}$ and $\psi^{n+1/2} = \frac{\psi^{n+1} + \psi^n}{2}$. In this system, the functions φ_k and ψ are defined on the closed curve Σ.

We can now apply the same technique to the conditions $\mathrm{ABC}_{1,P}^2$ and obtain

$$\begin{aligned}\partial_{\mathbf{n}}u - ie^{i\mathcal{V}}\sqrt{i\partial_t+\Delta_\Sigma}\left(e^{-i\mathcal{V}}u\right)+\frac{\kappa}{2}u \\ +(\partial_s\mathcal{V})e^{i\mathcal{V}}\left(i\partial_t+\Delta_\Sigma\right)^{-1/2}\partial_s\left(e^{-i\mathcal{V}}u\right) \\ -\frac{\kappa}{2}e^{i\mathcal{V}}\left(i\partial_t+\Delta_\Sigma\right)^{-1}\Delta_\Sigma\left(e^{-i\mathcal{V}}u\right)=0.\end{aligned}$$

The first terms of this equation are treated in a way similar as for $\mathrm{ABC}_{2,P}^2$. We have to introduce new auxiliary functions for lower order terms. The term $(\partial_s\mathcal{V})e^{i\mathcal{V}}\left(i\partial_t+\Delta_\Sigma\right)^{-1/2}\partial_s\left(e^{-i\mathcal{V}}u\right)$ is treated in two steps. First, we introduce a new auxiliary function η defined on Σ_T by

$$\left(i\partial_t+\Delta_\Sigma\right)^{1/2}\eta=\partial_s(e^{-i\mathcal{V}}u).$$

The second step consists in approximating the square-root operator by Padé approximants of order m

$$\left(\sum_{k=0}^m a_k^m\right)\eta-\sum_{k=1}^m a_k^m d_k^m\left(i\partial_t+\Delta_\Sigma+d_k^m\right)^{-1}\eta=\partial_s(e^{-i\mathcal{V}}u).$$

Next, we consider m new auxiliary functions $(\theta_k)_{1\le k\le m}$ defined on Σ_T by

$$\left(i\partial_t+\Delta_\Sigma+d_k^m\right)^{-1}\eta=\theta_k.$$

Similarly, we introduce the function ψ for the last term of $\mathrm{ABC}_{1,P}^2$, which satisfies on Σ the relation $i\partial_t\psi+\Delta_\Sigma\psi=\Delta_\Sigma\left(e^{-i\mathcal{V}}u\right)$. Thus, we get a system associated to the condition $\mathrm{ABC}_{1,P}^2$

$$\begin{cases}\partial_{\mathbf{n}}u - i\displaystyle\sum_{k=0}^m a_k^m u+\frac{\kappa}{2}u+ie^{i\mathcal{V}}\sum_{k=1}^m a_k^m d_k^m\varphi_k+(\partial_s\mathcal{V})e^{i\mathcal{V}}\eta \\ \qquad\qquad -\dfrac{\kappa}{2}e^{i\mathcal{V}}\psi=0, \quad \text{on } \Sigma_T, \\ \left(i\partial_t+\Delta_\Sigma+d_k^m\right)\varphi_k=e^{-i\mathcal{V}}u, \quad \text{on } \Sigma_T, \quad \text{for } 1\le k\le m, \\ \left(\displaystyle\sum_{k=0}^m a_k^m\right)\eta-\sum_{k=1}^m a_k^m d_k^m\theta_k=\partial_s\left(e^{-i\mathcal{V}}u\right), \quad \text{on } \Sigma_T, \\ \left(i\partial_t+\Delta_\Sigma+d_k^m\right)\theta_k=\eta, \quad \text{on } \Sigma_T, \quad \text{for } 1\le k\le m, \\ \left(i\partial_t+\Delta_\Sigma\right)\psi=\Delta_\Sigma\left(e^{-i\mathcal{V}}u\right), \quad \text{on } \Sigma_T, \\ \varphi_k(\mathbf{x},0)=\theta_k(\mathbf{x},0)=0 \quad \text{on } \Sigma, \quad \text{for } 1\le k\le m, \\ \psi(\mathbf{x},0)=0 \quad \text{on } \Sigma.\end{cases}$$

We deduce the following discretization

$$\begin{cases} \partial_{\mathbf{n}} v^{n+1} - i \sum_{k=0}^{m} a_k^m v^{n+1} + \frac{\kappa}{2} v^{n+1} + i e^{i\mathscr{W}^{n+1}} \sum_{k=1}^{m} a_k^m d_k^m \varphi_k^{n+1/2} \\ \qquad\qquad + \partial_s \mathscr{W}^{n+1} e^{i\mathscr{W}^{n+1}} \eta^{n+1/2} - \frac{\kappa}{2} e^{i\mathscr{W}^{n+1}} \psi^{n+1/2} = 0, \\ \left(\frac{2i}{\Delta t} + \Delta_\Sigma + d_k^m \right) \varphi_k^{n+1/2} - e^{-i\mathscr{W}^{n+1}} v^{n+1} = \frac{2i}{\Delta t} \varphi_k^n, \quad 1 \le k \le m, \\ \left(\sum_{k=0}^{m} a_k^m \right) \eta^{n+1/2} - \sum_{k=1}^{m} a_k^m d_k^m \theta_k^{n+1/2} = \partial_s \left(e^{-i\mathscr{W}^{n+1}} v^{n+1} \right), \\ \qquad\qquad\qquad\qquad\qquad\qquad\qquad\qquad \text{on } \Sigma_T, \\ \left(\frac{2i}{\Delta t} + \Delta_\Sigma + d_k^m \right) \theta_k^{n+1/2} - \eta^{n+1/2} = \frac{2i}{\Delta t} \theta_k^n, \quad 1 \le k \le m, \\ \left(\frac{2i}{\Delta t} + \Delta_\Sigma \right) \psi^{n+1/2} - \Delta_\Sigma \left(e^{-i\mathscr{W}^{n+1}} v^{n+1} \right) = \frac{2i}{\Delta t} \psi^n, \\ \varphi_k^0(\mathbf{x}) = \theta_k^0(\mathbf{x}) = 0 \quad \text{for } 1 \le k \le m, \quad \psi^0(\mathbf{x}) = 0 \quad \text{on } \Sigma. \end{cases} \tag{69}$$

Remark 3.4. . *When the potential and the computational domain are radially symetrical, the condition* $ABC_{1,P}^2$ *becomes*

$$\partial_{\mathbf{n}} u - i e^{i\mathcal{V}} \sqrt{i\partial_t + \Delta_\Sigma} \left(e^{-i\mathcal{V}} u \right) + \frac{\kappa}{2} u \\ - \frac{\kappa}{2} e^{i\mathcal{V}} \left(i\partial_t + \Delta_\Sigma \right)^{-1} \Delta_\Sigma \left(e^{-i\mathcal{V}} u \right) = 0, \quad \textit{on } \Sigma_T. \tag{70}$$

This leads to significant simplifications for the numerical treatment. In this case, the discretization reads

$$\begin{cases} \partial_{\mathbf{n}} v^{n+1} - i \sum_{k=0}^{m} a_k^m v^{n+1} + \frac{\kappa}{2} v^{n+1} + i e^{i\mathscr{W}^{n+1}} \sum_{k=1}^{m} a_k^m d_k^m \varphi_k^{n+1/2} \\ \qquad\qquad\qquad\qquad\qquad - \frac{\kappa}{2} e^{i\mathscr{W}^{n+1}} \psi^{n+1/2} = 0, \\ \left(\frac{2i}{\Delta t} + \Delta_\Sigma + d_k^m \right) \varphi_k^{n+1/2} - e^{-i\mathscr{W}^{n+1}} v^{n+1} = \frac{2i}{\Delta t} \varphi_k^n, \\ \qquad\qquad\qquad\qquad\qquad\qquad 1 \le k \le m, \\ \left(\frac{2i}{\Delta t} + \Delta_\Sigma \right) \psi^{n+1/2} - \Delta_\Sigma \left(e^{-i\mathscr{W}^{n+1}} v^{n+1} \right) = \frac{2i}{\Delta t} \psi^n, \\ \varphi_k(\mathbf{x}, 0) = 0 \quad \textit{for } 1 \le k \le m, \quad \psi^0(\mathbf{x}) = 0 \quad \textit{on } \Sigma. \end{cases} \tag{71}$$

Like in the one-dimensional case [4], it is not possible to give a proof of stability for these ABCs discretized with Padé approximants. A point of interest would be the study of stability for ABCs discretized using other rational approximations of the square root.

4. Finite element approximation and numerical results

The variational formulation for the semi-discretization (27) of the Schrödinger equation (1) consists in seeking the unknown function v^{n+1} in the Sobolev space $H^1(\Omega)$ such that for any test function $\psi \in H^1(\Omega)$, one has

$$\int_\Omega \left(\frac{2i}{\Delta t} v^{n+1}\psi - \nabla v^{n+1}\nabla\psi + W^{n+1}v^{n+1}\psi \right) d\Omega + \int_\Sigma \partial_{\mathbf{n}} v^{n+1}\psi d\Sigma = \int_\Omega \frac{2i}{\Delta t} u^n \psi d\Omega \quad (72)$$

The spatial approximation is realized by using the classical $\mathcal{P}_1$ finite element space of piecewise linear functions

$$V_h = \left\{ \varphi_h \in H^1(\Omega_h), \varphi_{h|T} \in \mathcal{P}_1, \forall T \in \mathcal{T}_h \right\},$$

where the bounded computational polygonal domain $\Omega_h = \cup_{T\in\mathcal{T}_h} T$ is constructed with the help of a regular triangulation $\mathcal{T}_h$. The curvature approximation is developed by a simple procedure [1] based only on the knowledge of the initial mesh. The finite element approximation space V_h being a subspace of $H^1(\Omega_h)$, the stability of the fully discrete scheme is simply a consequence of the stability of the semi-discrete scheme. At each time step, the resulting complex-valued sparse and symmetrical linear system is solved by a biconjugate gradient stabilized solver accelerated by an incomplete LU factorization preconditioner. The convergence is reached in only a few iterations.

We split our analysis in two parts, respectively for time independent and time dependent potentials. In both cases, we restrict ourselves to computations for which we have access to exact solutions. This allows us to compute error norm between an exact solution denoted by $u_{\text{ex}}(x, y, t)$ in the sequel and a numerical solution $u_{\text{num}}(x, y, t)$ equal to $u^n(x, y) \in V_h$ when $t \in [t_n, t_{n+1})$. An exact solution is given in term of solutions to the free Schrödinger equation

$$\begin{cases} i\partial_t v + \Delta v = 0, & (x, y) \in \mathbb{R}^2, t > 0 \\ v(x, y, 0) = v_0(x, y), & (x, y) \in \mathbb{R}^2, \end{cases} \quad (73)$$

where $v_0 \in L^2(\mathbb{R}^2)$. It is well-known that an exact solution of (73) can be obtained by convolution with the Green's kernel. When v_0 is a gaussian

$$v_0(x, y) = e^{-L(x^2+y^2)+i(k_1x+k_2y)}, \quad (74)$$

where $L > 0$ and $k = (k_1, k_2)^T$ is the wave vector, the exact solution is given by

$$v(x, y, t) = \frac{i}{i - 4Lt} \times \exp\left(-i \, \frac{L(x^2 + y^2) + i(k_1x + k_2y) + it(k_1^2 + k_2^2)}{i - 4Lt} \right). \quad (75)$$

4.1. Time independent potentials

The numerical simulations in this subsection are made for the repulsive quadratic potential $V_1(x,y,t) = \omega^2(x^2+y^2)$ (see Figures 3(a) and 3(b)). An explicit solution can be computed [12] in term of solution v of (73) by

$$u(x,y,t) = \exp\left(\frac{i\omega}{2}(x^2+y^2)\tanh(2\omega t)\right)\frac{v(\tilde{x},\tilde{y},\tilde{t})}{\cosh(2\omega t)} \tag{76}$$

where $\tilde{x} = x/\cosh(2\omega t)$, $\tilde{y} = y/\cosh(2\omega t)$ and $\tilde{t} = \tanh(2\omega t)/(2\omega)$. The computational domains Ω are p-balls

$$B_p(R) = \left\{(x,y)\in\mathbb{R}^2 \,|\, |x|^p + |y|^p \le R^p\right\}, 2 \le p < \infty,$$

which can be parameterized with respect to the angle θ by the relations

$$x(\theta) = R\,|\cos\theta|^{2/p}\cdot \mathrm{sg}(\cos\theta),$$
$$y(\theta) = R\,|\sin\theta|^{2/p}\cdot \mathrm{sg}(\sin\theta).$$

Obviously, we recover the usual circle of radius R for $p=2$. The interest of such a computational domain is that it becomes close to a square for large enough values of p while being smooth. We will use in this paper the two computational domains $\Omega_1 = B_2(0,2.5)$ and $\Omega_2 = B_8(0,2.5)$ represented on Figure 2. In all our computations, the final time is $T=1$. The main difference in the computations

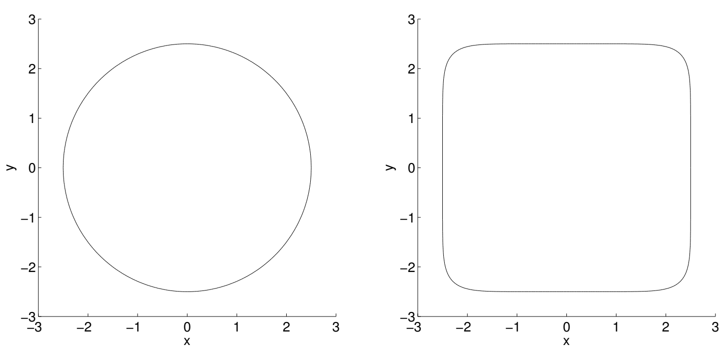

(a) $\Omega_1 = B_2(0,2.5)$ (b) $\Omega_2 = B_8(0,2.5)$

Figure 2: Computational domains Ω_1 and Ω_2

made on domain Ω_1 or Ω_2 is that the potential and curvature do not remain constant on their boundaries as we can notice it on Figure 3.

For a domain Ω_2 and a potential which are both radial, many simplifications occur in $\mathrm{ABC}_{1,T}^M$ and $\mathrm{ABC}_{1,P}^M$ for the gauge change approach. Indeed, the terms related to the derivative of $\mathcal{V}$ with respect to the curvilinear abscissa vanish in $\mathrm{ABC}_{1,T}^3$, $\mathrm{ABC}_{1,T}^4$ and $\mathrm{ABC}_{1,P}^2$, and the implementation greatly simplifies since the functions $e^{\pm i\mathcal{V}}$ are constant on Σ. When the domain or/and the potential are not symmetrical, no simplification can be made. As a consequence, the

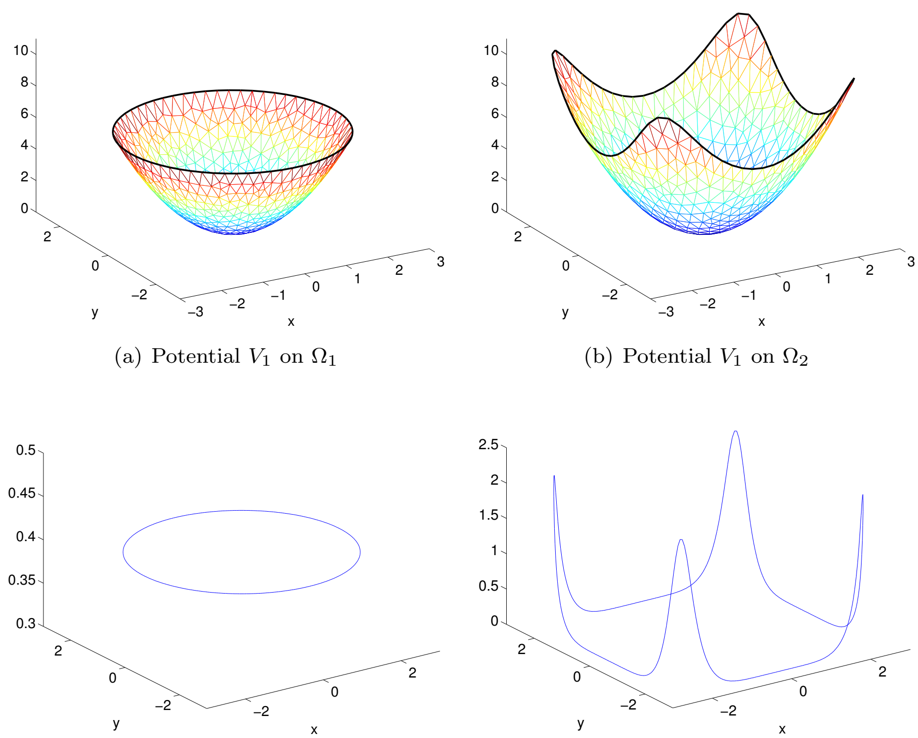

(a) Potential V_1 on Ω_1

(b) Potential V_1 on Ω_2

(c) Curvature on $\partial\Omega_1$

(d) Curvature on $\partial\Omega_2$

Figure 3: Potential and curvature for domains Ω_1 and Ω_2

computational cost is much more important, in particular for $\mathrm{ABC}_{1,T}^{M}$. The reason is that the discrete convolution imposes that the n finite element matrices depending on $e^{-i\mathcal{V}}$ must be rebuilt at the n-th time iteration.

The first experiments are made for the domain Ω_1 with $L = 4$ and $k = (0,0)^T$. The value of ω is 0.5. For this test case, we fix $\Delta t = 10^{-3}$. The domain Ω_1 is meshed with $423k = 423\,000$ triangles except for Fig. 5. In order to show the behavior of the various absorbing boundary conditions with respect to their order, we first plot the logarithm of the error norm $\|u_{\mathrm{ex}}(\cdot,t) - u_{\mathrm{num}}(\cdot,t)\|_{L^2(\Omega_1)}$ on Figure 4. As expected, the error decays with the order of the ABCs. Another interesting feature can be observed on Figure 5 where we report the evolution of the error with respect to the mesh size. We only keep the different highest order ABCs. We remark that the error always reaches the same limit for the different mesh sizes of Ω_1. Finally, we plot on Figure 6 the error norm for the best order of the different families of ABCs. The more convincing ABC is clearly the one obtained by the Taylor approximation in the framework of Strategy 1. The two Padé approaches give the same results in both strategies. The Taylor approach in Strategy 2 leads to the worst approximation. For completeness, we test the best ABC, namely $\mathrm{ABC}_{1,T}^{4}$, for long time simulations for a triangulation of Ω_1 involving $26k$ triangles. Indeed, from the previous curves, one may think that the error grows with respect to time. This is in fact not the case as it can be seen on Figure 7. The error remains almost constant for longer computational times.

The next simulations are performed on the domain Ω_2 which is meshed with $23k$ triangles. The time step Δt is chosen as $2 \cdot 10^{-3}$, the value of L remains unchanged but the wave vector is now $k = (3,3)^T$ and the value of ω is 1. This choice insures that the solution propagates in the direction of the lower left part of the domain which has the strongest curvature. Again, we plot the error norm for the various ABCs on Figure 8 and a comparison on Figure 9. The results confirm what we have already observed for Ω_1 but some differences appear concerning the behavior of the Padé approximation. The Padé approach for Strategy 1 gives better results than for Strategy 2. The best approach still consists in using $\mathrm{ABC}_{1,T}^{4}$. We next show on Figure 10 the evolution of the contour plot of the logarithm of $|u_{\mathrm{ex}}(\cdot,.)|$ and $|u_{\mathrm{num}}(\cdot,.)|$ for $\mathrm{ABC}_{1,T}^{4}$ which is satisfactory.

4.2. Time dependent potentials

As for the previous subsection, we have access to an explicit solution for $V_2(x,y,t) = f(t)(x^2+y^2)$ thanks to [12]. To this aim, we define two functions μ and ν solutions of the second-order ordinary differential equation

$$g''(t) - 4f(t)g(t) = 0$$

completed with initial data. Thereby, the function μ is solution to this ODE with $\mu(0) = 0$ and $\mu'(0) = 1$. Considering ν, one takes $\nu(0) = 1$ and $\nu(1) = 0$. Then, the solution is given by

$$u(x,y,t) = \frac{1}{\nu(t)} \exp\left(\frac{i}{4}\frac{\nu'(t)}{\nu(t)}\frac{x^2+y^2}{\nu(t)^2}\right) v\left(\frac{x}{\nu(t)}, \frac{y}{\nu(t)}, \frac{\mu(t)}{\nu(t)}\right).$$

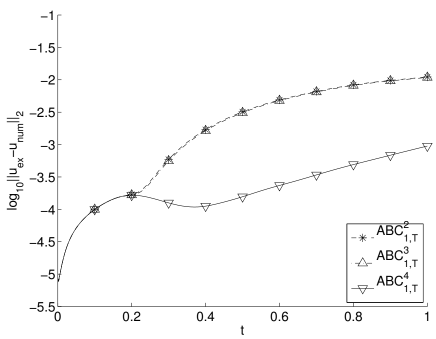

(a) $\mathrm{ABC}_{1,T}^{M}$

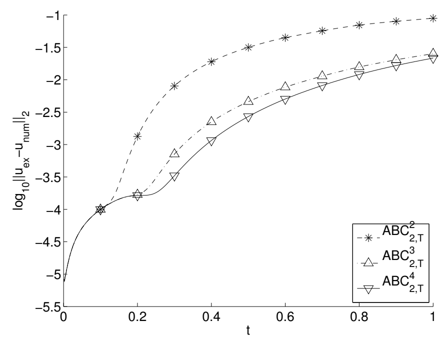

(b) $\mathrm{ABC}_{2,T}^{M}$

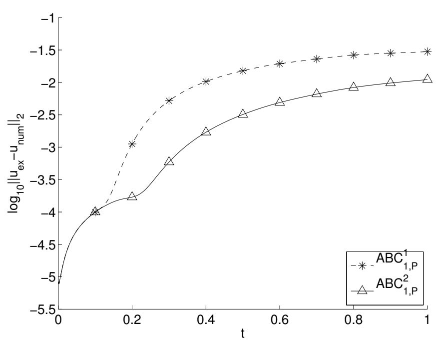

(c) $\mathrm{ABC}_{1,P}^{M}$

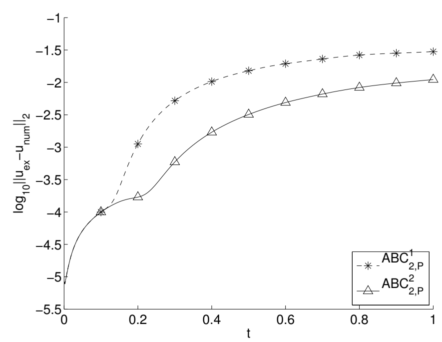

(d) $\mathrm{ABC}_{2,P}^{M}$

Figure 4: Evolution of the error norm $\log_{10}\left(\|u_{\mathrm{ex}}(\cdot,t)-u_{\mathrm{num}}(\cdot,t)\|_{L^2(\Omega_1)}\right)$ with respect to the ABC order.

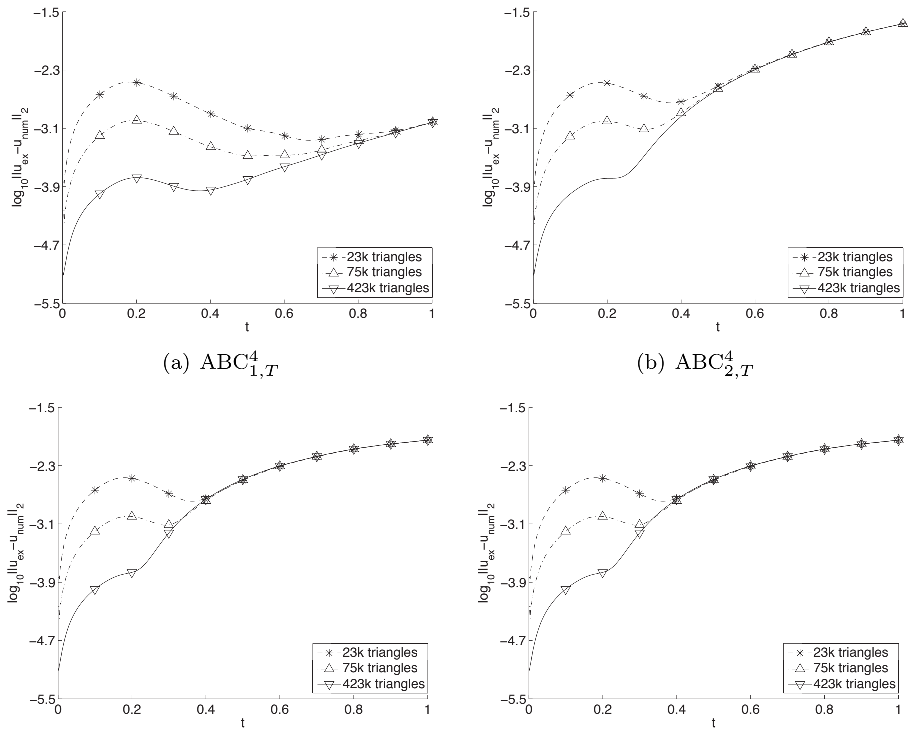

(a) $\mathrm{ABC}^4_{1,T}$ (b) $\mathrm{ABC}^4_{2,T}$

(c) $\mathrm{ABC}^2_{1,P}$ (d) $\mathrm{ABC}^2_{2,P}$

Figure 5: Evolution of the error norm $\log_{10}\left(\|u_{\mathrm{ex}}(\cdot,t)-u_{\mathrm{num}}(\cdot,t)\|_{L^2(\Omega_1)}\right)$ with respect to the mesh size.

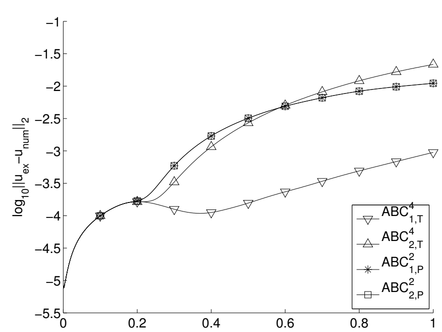

Figure 6: Comparison of the error norm $\log_{10}\left(\|u_{\mathrm{ex}}(\cdot,t)-u_{\mathrm{num}}(\cdot,t)\|_{L^2(\Omega_1)}\right)$ for different ABCs.

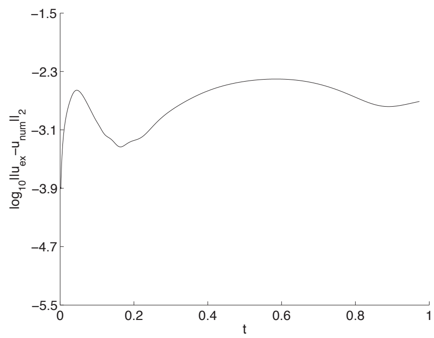

Figure 7: Error norm $\log_{10}\left(\|u_{\mathrm{ex}}(\cdot,t)-u_{\mathrm{num}}(\cdot,t)\|_{L^2(\Omega_1)}\right)$ for a long time computation for $\mathrm{ABC}^4_{1,T}$.

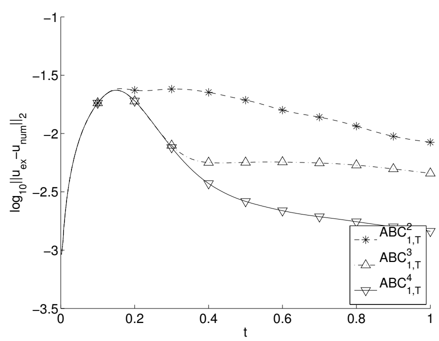

(a) $\mathrm{ABC}^M_{1,T}$

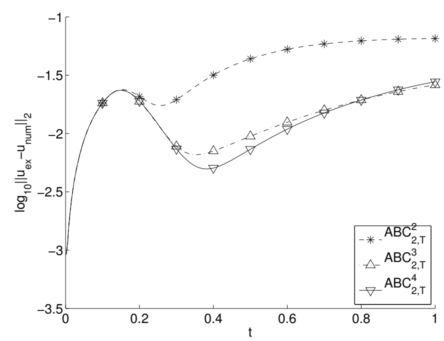

(b) $\mathrm{ABC}^M_{2,T}$

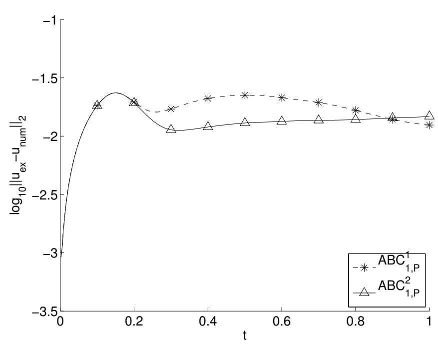

(c) $\mathrm{ABC}^M_{1,P}$

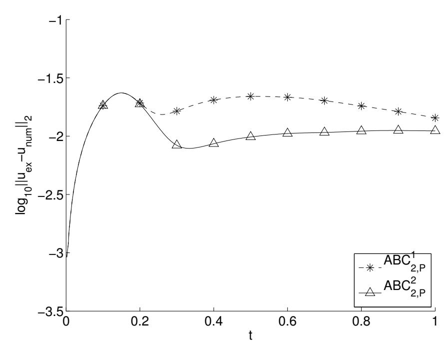

(d) $\mathrm{ABC}^M_{2,P}$

Figure 8: Evolution of the error norm $\log_{10}\left(\|u_{\mathrm{ex}}(\cdot,t)-u_{\mathrm{num}}(\cdot,t)\|_{L^2(\Omega_2)}\right)$ with respect to the ABC order.

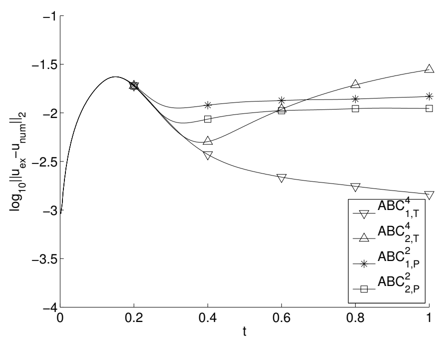

Figure 9: Comparison of the error norm $\log_{10}\left(\|u_{\mathrm{ex}}(\cdot,t)-u_{\mathrm{num}}(\cdot,t)\|_{L^2(\Omega_2)}\right)$ for different ABCs.

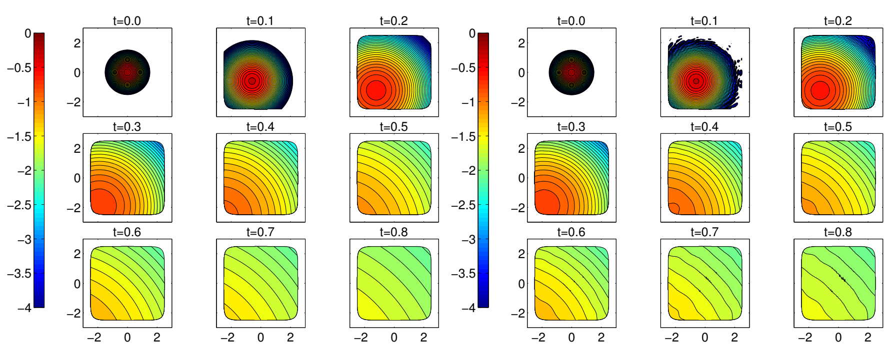

Figure 10: Evolution of the contour of $\log_{10}|u_{\mathrm{ex}}(\cdot,t)|$ (left) and $\log_{10}|u_{\mathrm{num}}(\cdot,t)|$ (right) for $L=4$, $k=(3,3)^T$ on Ω_2.

If the function f is linear, $f(t) = \alpha t$, the solution is explicitely given by using Airy's special functions Ai and Bi. Then, setting, $\tilde{t} = 2^{2/3}\alpha^{1/3}t$, we get

$$\mu(t) = 2^{1/3}\frac{\pi}{6\alpha^{1/3}\Gamma(2/3)}\left(3^{1/3}Bi(\tilde{t}) - 3^{5/6}Ai(\tilde{t})\right)$$

and

$$\nu(t) = \frac{1}{2}\Gamma(2/3)\left(3^{2/3}Ai(\tilde{t}) + 3^{1/6}Bi(\tilde{t})\right).$$

The numerical experiments are made on Ω_1 meshed with $105k$ triangles. The time step Δt is chosen as $2 \cdot 10^{-3}$ and the function f is $f(t) = (1 - \cos(2\pi t))/2$. The parameters of the solution are $L = 4$, $k = (0,0)^T$ and $\omega = 1$. As in the previous subsection, we plot the evolution of the error norm for the different ABCs on Figure 11 and compare the results on 12. The conclusions remain unchanged and the best ABC is still $\mathrm{ABC}^4_{1,T}$.

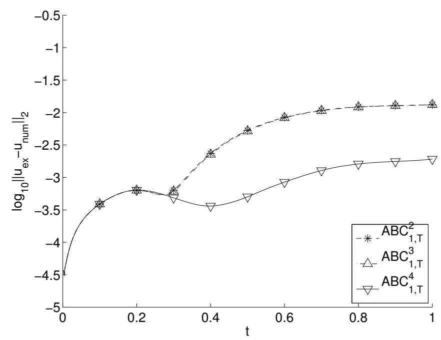

(a) $\mathrm{ABC}^M_{1,T}$

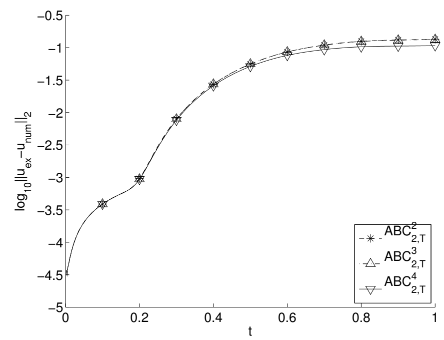

(b) $\mathrm{ABC}^M_{2,T}$

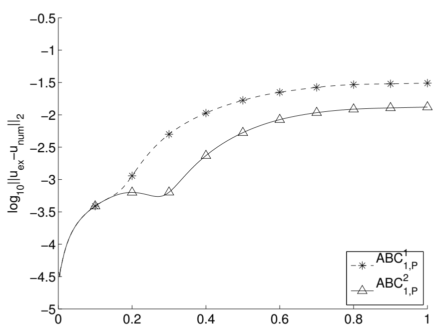

(c) $\mathrm{ABC}^M_{1,P}$

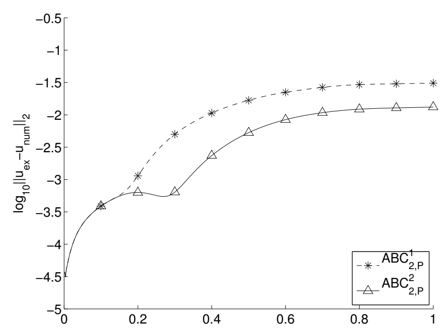

(d) $\mathrm{ABC}^M_{2,P}$

Figure 11: Evolution of the error norm $\log_{10}\left(\|u_{\mathrm{ex}}(\cdot,t) - u_{\mathrm{num}}(\cdot,t)\|_{L^2(\Omega_1)}\right)$ with respect to the ABCs order.

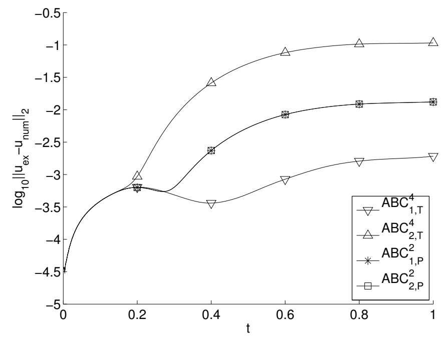

Figure 12: Comparison of the error norm $\log_{10}\left(\|u_{\mathrm{ex}}(\cdot,t)-u_{\mathrm{num}}(\cdot,t)\|_{L^2(\Omega_1)}\right)$ for the different ABCs.

5. Conclusion

The aim of this paper was to propose suitable discretization schemes of ABCs proposed in [6]. Furthermore, stability results have been proved in some cases. Numerical simulations are provided to compare the different kinds of ABCs. It appears that the most accurate ABC is $\mathrm{ABC}^4_{1,T}$ which is related to the application of Taylor's expansion to the first strategy of construction of ABCs based on a gauge change. Acceleration of the evaluation of the fractional operators [25] involved in the definition of this ABC should strongly improve the overall computational cost of their application but is however beyond the scope of our paper. Finally, let us remark that our developments can be *a priori* extended to the three-dimensional case for smooth surfaces and by using related differential geometry tools. However, the computation of the symbols, already heavy in the two-dimensional situation, would be very long and tedious. Furthermore, the numerical simulations would also bring technical challenges, linked e.g. to mesh generation and the resolution of large scale linear systems.

A. $\mathcal{Z}$-transform: technical annex

For the sake of clarity, we precise some notations and results about the $\mathcal{Z}$-transform of a discrete signal [14].

Definition A.1. *Let $(f_n)_{n\in\mathbb{N}}$ be a discrete signal. We call $\mathcal{Z}$-transform of (f_n), and we denote by $\mathcal{Z}(f_n)$ or $\hat{f}$, the function of the z variable defined by*

$$\hat{f}(z)=\mathcal{Z}(f_n)(z)=\sum_{n=0}^{+\infty} f_n z^{-n}, \qquad \text{for } |z|>\hat{R}_f, \tag{77}$$

where $\hat{R}_f$ denotes the convergence radius of the series $\hat{f}$ which is defined by

$$\hat{R}_f=\inf\left\{R>0\ ;\ \sum_n f_n R^{-n}<+\infty\right\}. \tag{78}$$

Thereby, $\hat{R}_f$ is the inverse of the convergence radius of the power series $\sum f_n z^n$.

We denote by $\star$ the usual convolution product

$$a_n \star b^n = (a \star b)_n = \sum_{k=0}^{n} a_k b^{n-k}.$$

Let us recall some classical properties of the $\mathcal{Z}$ transform.

Proposition A.1. *Let $(f_n)_{n\in\mathbb{N}}$ and $(g_n)_{n\in\mathbb{N}}$ be two discrete signals with convergence radius $\hat{R}_f$ and $\hat{R}_g$, respectively. Then, the following results hold*

1. $\mathcal{Z}(f_{n+1}) = z\hat{f} - zf(0)$,
2. $\mathcal{Z}(f_{n+1} \pm f_n) = (z \pm 1)\hat{f}(z) - zf(0)$,
3. $\mathcal{Z}(f_n \star g_n) = \hat{f}(z)\hat{g}(z)$, *for* $|z| > \max(\hat{R}_f, \hat{R}_g)$.

We also have the following lemma used in the stability proofs of the paper.

Lemma A.1. *Let $(u_p)_{p\in\mathbb{N}}$ and $(h_p)_{p\in\mathbb{N}}$ be two sequences. We define the sequence $(y_p)_{p\in\mathbb{N}}$ by*

$$y_p = \sum_{k=0}^{p} h_k u_{p-k},$$

and by $\hat{h}$ the $\mathcal{Z}$-transform of $(h_p)_{p\in\mathbb{N}}$, for which we assume that $R_{\hat{h}} \geq 1$. Let $\mathbb{H}(\mathbb{E})$ be the Hardy space on $\mathbb{E} = \{z \in \mathbb{C}, |z| > 1\}$

$$\mathbb{H}(\mathbb{E}) = \left\{ \mathcal{H} \text{ holomorphic on } \mathbb{E} \text{ s.t. } \sup_{r>1} \int_{-\pi}^{\pi} \left|\mathcal{H}(re^{i\omega})\right| d\omega < +\infty \right\}.$$

If $\hat{h} \in \mathbb{H}(\mathbb{E})$, then one has

$$\sum_{p=0}^{n} \overline{u_p} y_p = \frac{1}{2\pi} \int_{-\pi}^{\pi} \hat{h}(e^{i\omega}) \left| \sum_{p=0}^{n} u_p e^{-i\omega p} \right|^2 d\omega. \tag{79}$$

Proof. Let us define, for $\rho \geq 1$, $y_p(\rho) = \sum_{k=0}^{p} h_k \rho^{-k} u_{p-k}$. We fix $n < \infty$ and consider the Laurent polynomials $\hat{y}_\rho(z) := \sum_{p=0}^{n} y_p(\rho) z^{-p}$ and $\hat{u}(z) := \sum_{p=0}^{n} u_p z^{-p}$. By using the Cauchy product, one has for all z s.t. $|z| > \rho$

$$\hat{h}(\rho z) \cdot \hat{u}(z) = \hat{h}_\rho(z) + \sum_{p=n+1}^{\infty} \left(\sum_{k=p-n}^{p} h_k \rho^{-k} u_{p-k} \right) z^{-p}.$$

In particular, this is true for the unit circle. We compute the L^2 scalar product on the unit circle for the measure $\frac{1}{2\pi} d\omega$. The orthogonality of z^p implies that

$$\left\langle \hat{u}, \hat{h} \cdot \hat{u} \right\rangle = \langle \hat{u}, \hat{y}_\rho \rangle = \sum_{p=0}^{n} \overline{u_p} y_p(\rho).$$

The left hand side of this equality is reduced to

$$\frac{1}{2\pi}\int_{-\pi}^{\pi}\hat{h}(\rho e^{i\omega})\left|\sum_{p=0}^{n}u_p e^{-i\omega p}\right|^2\,d\omega.$$

But, $\hat{h}(\rho e^{i\omega})$ converges to $\hat{h}(e^{i\omega})$ in L^1 when $\rho\to 1^+$. Therefore, since $\lim_{\rho\to 1^+} y_p(\rho) = y_p$, this ends the proof of Lemma A.1. $\square$

This lemma is mainly used in the following result.

Lemma A.2. *Let $(\alpha_n)_n$, $(\beta_n)_n$ and $(\gamma_n)_n$ be the sequences given by (31), and $(\varphi^k)_{k\in\mathbb{N}}$ a sequence of complex numbers. We have the following properties:*

$$Q_\alpha = \sum_{p=0}^{n}\overline{\varphi^p}\sum_{k=0}^{p}\alpha_{p-k}\varphi^k \ \in e^{i\pi/4}\mathbb{R}^+\cup e^{-i\pi/4}\mathbb{R}^+, \tag{80}$$

$$Q_\beta = \sum_{p=0}^{n}\overline{\varphi^p}\sum_{k=0}^{p}\beta_{p-k}\varphi^k \ \in e^{i\pi/4}\mathbb{R}^+\cup e^{-i\pi/4}\mathbb{R}^+, \tag{81}$$

$$Q_\gamma = \sum_{p=0}^{n}\overline{\varphi^p}\sum_{k=0}^{p}\gamma_{p-k}\varphi^k \ \in \{\mathrm{Re}(z)\geq 0\}. \tag{82}$$

Proof. The proof of the result for the terms Q_α and Q_β mainly relies on Lemma A.1 (see Annex A). Let us consider here Q_α (the proof is similar for Q_β). The $\mathcal{Z}$-transform of the sequence $(\alpha_n)_n$ evaluated on the unit circle for $\omega\in(-\pi,\pi)$ is given by $\hat{\alpha}(e^{i\omega}) = \sqrt{\frac{e^{i\omega}+1}{e^{i\omega}-1}} \in L^1(-\pi,\pi)$. It is easy to see that $\hat{\alpha}\in\mathbb{H}(\mathbb{E})$. Therefore, Lemma A.1 holds and we have

$$Q_\alpha = \frac{1}{2\pi}\int_{-\pi}^{\pi}\sqrt{\frac{e^{i\omega}+1}{e^{i\omega}-1}}\left|\sum_{n=0}^{P}v^n e^{-i\omega n}\right|^2 d\omega.$$

But for $\omega\in(-\pi;\pi)$, one has $\sqrt{\frac{e^{i\omega}+1}{e^{i\omega}-1}} = \sqrt{i\tan\left(\frac{\omega}{2}\right)}$. Hence, the application $z\mapsto\sqrt{\frac{z+1}{z-1}}$ maps the unit circle onto $e^{i\pi/4}\mathbb{R}^+\cup e^{-i\pi/4}\mathbb{R}^+$. This implies that

$$Q_\alpha\in e^{i\pi/4}\mathbb{R}^+\cup e^{-i\pi/4}\mathbb{R}^+.$$

This proof cannot be extended to Q_γ since the $\mathcal{Z}$-transform of the sequence $(\gamma_n)_n$ evaluated on the unit circle for $\omega\in(-\pi,\pi)$ does not belong to $\mathbb{H}(\mathbb{E})$. We therefore proceed in a different way. The term Q_γ can be interpreted as an hermitian form

$$Q_\gamma = \sum_{p=0}^{n}\overline{\varphi^p}\left(\gamma_p\star\varphi^p\right) = {}^t\overline{\boldsymbol{\varphi}}A\boldsymbol{\varphi} = \langle\boldsymbol{\varphi},A\boldsymbol{\varphi}\rangle$$

where $\boldsymbol{\varphi}$ is the vector with size $n+1$ and complex coefficients $\boldsymbol{\varphi} = (\varphi_0, \cdots, \varphi_n)^T$ and A designates the real coefficients matrix of size $(n+1) \times (n+1)$ defined by

$$A = \begin{pmatrix} 1 & 0 & \dots & \dots & 0 \\ 2 & 1 & \ddots & & \vdots \\ 2 & 2 & 1 & \ddots & \vdots \\ \vdots & & \ddots & \ddots & 0 \\ 2 & \dots & \dots & 2 & 1 \end{pmatrix}.$$

Since A is positive, for any real valued vector $\mathbf{x}$ we have

$$\langle \mathbf{x}, A\mathbf{x} \rangle \geq 0.$$

We now decompose the complex valued vector $\boldsymbol{\varphi}$ as $\boldsymbol{\varphi} = \mathbf{x} + i\mathbf{y}$, with $\mathbf{x}$ and $\mathbf{y}$ two real valued vectors. We compute the hermitian product

$$Q_\gamma = \langle \boldsymbol{\varphi}, A\boldsymbol{\varphi} \rangle = \langle \mathbf{x}, A\mathbf{x} \rangle + \langle \mathbf{y}, A\mathbf{y} \rangle + i\big[\langle \mathbf{x}, A\mathbf{y} \rangle - \langle \mathbf{y}, A\mathbf{x} \rangle\big].$$

Then we have

$$\mathrm{Re}(Q_\gamma) = \langle \mathbf{x}, A\mathbf{x} \rangle + \langle \mathbf{y}, A\mathbf{y} \rangle \geq 0,$$

and

$$\mathrm{Im}(Q_\gamma) = \langle \mathbf{x}, A\mathbf{y} \rangle - \langle \mathbf{y}, A\mathbf{x} \rangle,$$

this term being non null if $\mathbf{x}$ or $\mathbf{y}$ are not equal to zero since A is not symmetric. Consequently, we have

$$Q_\gamma \in \{\mathrm{Re}(z) \geq 0\}.$$

$\square$

Acknowledgements. The authors want to thank professor J.-F. Burnol for his valuable help concerning the proof of Lemma A.1.

References

[1] X. Antoine, Fast approximate computation of a time-harmonic scattered field using the On-Surface Radiation Condition method, *IMA J. Appl. Math.* 66 (2001), pp. 83-110.

[2] X. Antoine, A. Arnold, C. Besse, M. Ehrhardt, and A. Schädle, A review of transparent and artificial boundary conditions techniques for linear and nonlinear Schrödinger equations, *Commun. Comput. Phys.*, **4** n°4 (2008) 729–796.

[3] X. Antoine and C. Besse. Unconditionally stable discretization schemes of non-reflecting boundary conditions for the one-dimensional Schrödinger equation. *J. Comput. Phys.*, **188** n°1 (2003) 157–175.

[4] X. Antoine, C. Besse, and P. Klein. Absorbing boundary conditions for the one-dimensional Schrödinger equation with an exterior repulsive potential. *J. Comput. Phys.*, **228** n°2 (2009) 312–335.

[5] X. Antoine, C. Besse, and P. Klein. Absorbing boundary conditions for Schrödinger equations with general potentials and nonlinearities, *SIAM J. Sci. Comput.*, **33** n°2 (2011) 1008–1033.

[6] X. Antoine, C. Besse, and P. Klein. Absorbing boundary conditions for the two-dimensional Schrödinger equation with an exterior potential. Part I: construction and *a priori* estimates. *M3AS*, **22** n°10 (2012) 38 pages, DOI: 10.1142/S0218202512500261.

[7] X. Antoine, C. Besse, and V. Mouysset. Numerical schemes for the simulation of the two-dimensional Schrödinger equation using non-reflecting boundary conditions. *Math. Comp.*, **73** n°248 (2004) 1779–1799.

[8] R. Carles. Linear vs. nonlinear effects for nonlinear Schrödinger equations with potential. *Commun. Contemp. Math.*, **7** n°4 (2005) 483–508.

[9] T. Cazenave. *An introduction to nonlinear Schrödinger equations.* Instituto de Matemática-UFRJ, Rio de Janeiro, RJ, (1996).

[10] P. Debernardi and P. Fasano. Quantum confined Stark effect in semiconductor quantum wells including valence band mixing and Coulomb effects. *IEEE Journal of Quantum Electronics*, **29** (1993) 2741–2755.

[11] A. del Campo, G. Garcia-Calderon, and J. G. Muga. Quantum transients. *Physics Report-Review Section of Physics Letters*, **476** (1-3):1–50, (2009).

[12] R. Carles Nonlinear Schrödinger equation with time dependent potential. *Commun. Math. Sci.*, **9** n°4 (2011) 937–964.

[13] B. Engquist and A. Majda. Absorbing boundary conditions for the numerical simulation of waves. *Math. Comp.*, **31** n°139 (1977) 629–651.

[14] G. Doetsch, *Anleitung zum praktischen Gebrauch der Laplace–Transformation und der Z–Transformation*, R. Oldenburg Verlag München, Wien, 3. Auflage 1967.

[15] B. Engquist and A. Majda. Radiation boundary conditions for acoustic and elastic wave calculations. *Comm. Pure Appl. Math.*, **32** n°3 (1979) 313–357.

[16] P. Klein. *Construction et analyse de conditions aux limites artificielles pour des équations de Schrödinger avec potentiels et non linéarités.* Ph.D. Thesis, Université H. Poincaré, Nancy, November 2010 `http://tel.archives-ouvertes.fr/tel-00560706/fr/`.

[17] M. Levy. Non-local boundary conditions for radiowave propagation. *Phys. Rev. E*, **62** n°1 (2000) 1382–1389.

[18] M. Levy. *Parabolic equation methods for electromagnetic wave propagation*, volume 45 of *IEE Electromagnetic Waves Series*. Institution of Electrical Engineers (IEE), London, (2000).

[19] E. Lorin, A. Bandrauk, and S. Chelkowski. Numerical Maxwell-Schrödinger model for laser-molecule interaction and propagation. *Comput. Phys. Comm.*, **177** n°12 (2007) 908–932.

[20] E. Lorin, A. Bandrauk, and S. Chelkowski. Mathematical modeling of boundary conditions for laser-molecule time dependent Schrödinger equations and some aspects of their numerical computation-One-dimensional case. *Numer. Meth. for P.D.E.*, **25** (2009) 110–136.

[21] E. Lindmann. Free-space boundary conditions for the time dependent wave equation. *J. Comput. Phys.*, 18:16–78, 1985.

[22] F. Milinazzo, C. Zala, and G. Brooke. Rational square-root approximations for parabolic equation algorithms. *J. Acoust. Soc. Amer.*, 101 (2):760–766, 1997.

[23] J. G. Muga, J. P. Palao, B. Navarro, and I. L. Egusquiza. Complex absorbing potentials. *Phys. Rep.*, **395** n°6 (2004) 357–426.

[24] C. Zheng. An exact absorbing boundary condition for the Schrödinger equation with sinusoidal potentials at infinity. *Commun. Comput. Phys.*, **3** n°3 (2008) 641–658.

[25] C. Zheng. Fast evaluation of exact transparent boundary condition for one-dimensional cubic nonlinear Schrödinger equation. *Front. Math. China*, **5** n°3 (2010) 589–606.